IBM Journal of Research and Development
Volume 43, Numbers 1/2, 1999
Plasma processing

Table of contents: HTML ASCII
This article: HTML ASCII DOI: 10.1147/rd.431.0127

Plasma-assisted oxidation, anodization, and nitridation of silicon

by D. W. Hess

Plasma-assisted oxidation, anodization, and nitridation of silicon have been performed in microwave, rf, and dc plasmas with a variety of reactor configurations and a range of plasma densities. Compared to thermal processes at equivalent substrate temperatures, film growth rates are accelerated by the plasma-enhanced generation of reactive chemical species or by the presence of electric fields to aid charged-particle transport during plasma processes. Oxidation, anodization, and nitridation kinetics, mechanisms, and film properties attainable with plasma enhancement are discussed for crystalline, polycrystalline, and amorphous silicon layers and for silicon-germanium alloys. The use of these plasma methods for surface and interface modification of silicon-based materials and devices is described.

Introduction

In order to reduce the thermal budget in the fabrication of current and future microelectronic devices and integrated circuits (ICs), high-temperature process steps must be minimized in number and duration, or low-temperature alternatives invoked. Similarly, the fabrication of thin-film transistors (TFTs) for flat-panel displays requires low temperatures because of the presence of glass substrates. As a result of the extensive use and criticality of silicon oxidation in the production of these silicon-based devices and circuits, several approaches to low-temperature (<600°C) oxidation at reasonable rates have been explored. These approaches include the use of high pressures, rapid thermal processing (RTP), and plasma-assisted oxidation. Similarly, the excellent barrier properties of silicon nitride, combined with the higher (compared to silicon dioxide) dielectric constant, have fueled efforts to find low-temperature alternatives to direct thermal growth of silicon nitride on silicon surfaces. Again, RTP and plasma-assisted methods have been investigated as possible techniques to achieve such low-temperature growth.

Owing to the low temperatures required in comparison to RTP, plasma-assisted silicon oxidation methods have received considerable attention [1-8]. Clearly, oxidation or nitridation performed at temperatures below 600°C reduces dopant diffusion, interdiffusion of thin films, and defect generation compared to higher-temperature thermally driven processes. Such considerations are equally important, if not more so, to the oxidation of silicon-germanium alloys. Furthermore, the presence of an electric field in these processes can enhance the directionality of

oxidation, thereby minimizing or eliminating bird's-beak formation during local oxidation steps.

In this paper, various approaches to the plasma-assisted oxidation and nitridation of crystalline, polycrystalline, and amorphous silicon and silicon- germanium alloys are compared and contrasted, including the use of dc, rf, microwave, and high-density (e.g., electron cyclotron resonance and helical resonator) discharges. In addition, related studies that permit nano- oxidation (e.g., scanning tunneling microscopy and atomic force microscopy) are noted and commonalities with plasma methods described. Emphasis is on the kinetics and mechanistic aspects of film growth and on the resulting film properties.

Plasma oxidation and anodization of single-crystal silicon

When a silicon substrate in contact with a plasma is at floating potential during oxidation, the process is generally called plasma oxidation; when an external (positive) bias is applied to the substrate, the process is termed anodization. The difference between these plasma processes and thermal oxidation is that in most plasma reactor configurations, silicon and the growing silicon dioxide layer are exposed to reactive ions, electrons, atomic oxygen species, and UV, deep-UV, and even X-ray radiation (depending upon the plasma source) during oxidation. Electric fields, either externally applied or generated internally from charge buildup in the growing film or on the film surface, are also important in that they greatly affect the charged-particle (ion, electron) transport from the plasma to the oxide surface and through the oxide layer. In plasma oxidation or anodization, oxidant transport across the growing oxide layer often controls the oxidation rate. In many cases, the externally applied fields can be substantial (>1 MV/cm). These factors combine to yield plasma-assisted oxidation rates at low pressures (<1 Torr) and temperatures (<600°C) equal to those of dry oxygen at atmospheric pressure and temperatures >900°C.

It is important to note that changes in plasma parameters (e.g., pressure, power, frequency) and reactor design alter the electron concentration and anodization current, thereby changing the oxidant flux to the silicon-silicon dioxide interface. Thus, direct comparison of oxidation kinetics and film properties arising from different reactor systems is difficult unless carefully defined parametric information is available. For example, as a result of the relatively high power levels and low pressures used in high-density plasmas, high-energy photon exposure and film heating by high current densities can affect oxidation rates as well as the generation and annihilation of oxide charges and interface states. In addition, variations in current density due to undefined substrate/substrate holder areas can yield different oxidation results in otherwise similar reactor configurations.

• *Microwave plasmas*

The earliest studies of silicon oxidation using microwave discharges (2.45 GHz) were reported in the mid-1960s [9, 10] ; a generic reactor configuration is shown in **Figure 1**. These studies indicated that oxidation rates of silicon samples immersed in the discharge scaled with plasma density [10] and that oxidation rates were enhanced significantly under positive substrate bias conditions [9, 10]. Such observations suggested that negatively charged species transport during anodization was important. Although exact substrate temperatures were not

reported, current densities were approximately 20 mA/cm^2 at 0.6 Torr O_2 [9] and 100 mA/cm^2 at 0.15 Torr [10] ; under these conditions, oxide thicknesses in excess of 400 nm were grown in one hour with the application of a positive bias. As-grown films displayed aqueous HF etch rates and refractive indices identical to those of thermally grown SiO_2, with a mean breakdown field (MBDF) of 3-7 MV/cm, compared to 5-10 MV/cm for thermally grown oxides [10]. Furthermore, the high-frequency capacitance-voltage (CV) curves exhibited small flat-band shifts to negative voltage upon negative bias-temperature stress [10].

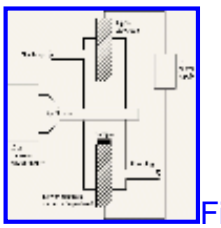
Figure 1

A reactor configuration similar to that shown in Figure 1 was used to investigate the kinetics of silicon anodization, using both microwave and rf (27 MHz) excitation at 500°C [11-14]. At 0.1 Torr O_2, the oxidation rate correlated with the gas-phase flux of O^- to the substrate surface, as suggested by mass spectrometer studies. Constant current and constant voltage anodizations yielded initial linear growth rates which were controlled by the concentration of O^- in the plasma. This process was followed by a space-charge-limited transport of O^- during which the growth rate approached parabolic behavior at longer anodization times. At current densities above 7 mA/cm^2 (apparently based on substrate area), an O_2 pressure of 100 mTorr, and a substrate temperature of 580°C, microwave plasma oxidation yielded growth rates in excess of 300 nm/hr. Although space- charge control was invoked to analyze the oxidation kinetics, the measured overall oxide field as a function of oxide thickness obeyed Ohm's law. As-grown effective oxide charge density was ~8 x 10^{11} cm^{-2}, with mobile charge levels in the range 1-3 x 10^{11} cm^{-2} and MBDF in the 5-8-MV/cm range [14]. After a 480°C post-metallization forming-gas anneal, the effective oxide charge density dropped to ~5 x 10^{11} cm^{-2}. Similar results were obtained with rf excitation, but lower anodization rates were o bserved, apparently due to lower concentrations of O^- in the plasma atmosphere.

Using a reactor design similar to that shown in Figure 1, but configured so that the anodization current was essentially confined with a quartz tube to a specific substrate surface area, silicon oxidation was performed at ~55 mTorr O_2, ~10 mA/cm^2, and a substrate temperature of ~400°C [15]. A constant growth rate of ~1.4 nm/min was observed up to four hours (~350 nm) oxidation time (**Figure 2**). This result is in opposition to the previously discussed microwave studies, and suggests that growth is controlled by field- assisted ionic conduction (negatively charged oxygen species) rather than by diffusion (parabolic relationship). It is likely that such discrepancies are due to higher current densities in Reference [15] than in References [9-14], where the area of current flow is not defined by physical restrictions. Thus, at (intentional or unintentional) low current densities, where growth rates are more controlled by temperature than by current, parabolic or linear-parabolic kinetics may dominate (e.g., Reference [14]), and activation energies are

therefore higher (0.31 eV for parabolic region) than for current-controlled growth (0.06 eV for ohmic region [15]). Chlorine addition also improved oxide electrical properties; after a post-metallization forming-gas anneal, the effective charge level was ~5 x 10^{10} cm^{-2}, with a mobile charge density of ~2 x 10^{10} cm^{-2} and a MBDF of 10 MV/cm [14].

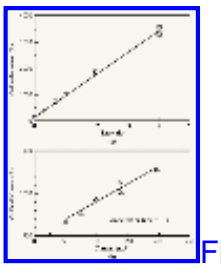
Figure 2

Isotopic labeling studies using ^{18}O plasma oxidation of an existing thermally grown SiO_2 film on silicon indicated that without anodization current, only the surface layer of oxide was enriched in ^{18}O; when plasma anodization was performed, ^{18}O was detected at the SiO_2 surface and at the Si-SiO_2 interface [15]. A linear dependence of growth rate on current was noted, while no difference in growth rates between (100) and (111) silicon was observed [15]. At an anodic current density of 14.1 mA/cm^2 and a temperature range of 230° to 405°C, an activation energy of 0.06 eV was calculated [15]. The above results are consistent with an oxidation process controlled by the field-assisted transport of ionic species, rather than by thermal reaction kinetics or concentration gradient diffusion. To date, no clear evidence exists indicating that silicon species are transported into the growing oxide layer; thus, plasma anodization appears to occur by field-aided oxygen ion transport to the Si-SiO_2 interface.

In an attempt to increase the oxidation rate and improve the oxide electrical properties, chlorine-containing gases such as trichloroethylene (TCE) or chlorine have been added to the anodization atmosphere [14]. With TCE additions to O_2, the oxidation rate increased at additions below 4% TCE; the reasons for this increase are not clear, but the authors speculate that an enhancement of the O^- concentration may be involved. Alternatively, chlorine or chlorine-containing species (e.g., Cl, Cl_2, or HCl) could assist bond-breaking at the Si-SiO_2 interface. At TCE additions of ~8% [14], the effective charge and mobile oxide charge were minimized after a post-metallization forming-gas anneal (~5 x 10^{11} cm^{-2} and ~3 x 10^{-10} cm^{-2}, respectively), and the MBDF was ~10 MV/cm, with a narrow breakdown distribution; similar results were observed for Cl_2 additions. Such observations are analogous to those reported for high-temperature thermal oxidation with chlorine additions [16].

Oxidation of silicon in downstream afterglows of high pressure (1-11 Torr) microwave-induced oxygen plasmas has been invoked [17-21] in an attempt to minimize the intense radiation exposure of substrates that occurs in the configurations described above. Since silicon substrates were not in direct contact with the plasma in afterglow systems, only neutral or possibly excited-state oxygen atoms or oxygen molecules reached the surface of the growing oxide layer. The reactors utilized were similar to that shown in Figure 1, but the substrate was placed outside the glow region and no external bias was applied. Oxidation rates under

these conditions were at least one order of magnitude lower than those observed within the discharge region. The oxidation appeared to be transport-limited for all thicknesses, despite the thin oxides formed (<12 nm in one hour at temperatures below 800°C). Rates were enhanced by increasing the gas-phase atomic oxygen concentration either by increasing the pressure or by optimizing the amount of argon added to the O_2 atmosphere; at 575°C, this corresponded to 85% Ar [18, 19]. These results indicated that atomic oxygen, generated in the gas phase, was the primary oxidant. Although the rates were low (14 nm in four hours at 7 Torr), they were considerably higher than thermal oxidation rates at atmospheric pressure and the same temperature.

Similarly, oxidation of silicon with O_2/N_2 discharges in the temperature range of 600° to 800°C without externally applied bias resulted in an enhancement of the oxidation rate over that for O_2 [20, 21]. In one hour at 750°C and 1 Torr of 5% N_2 in O_2, the oxide thickness increased from 7 nm (pure O_2) to 11 nm. The addition of N_2 decreased the effective activation energy for oxidation from 1.15 eV to 0.71 eV, but parabolic oxidation kinetics were observed in both oxidation ambients. Mass spectrometer studies indicated that NO was formed in the O_2/N_2 plasma, suggesting that the enhanced oxidation rate was related to a change in the primary oxidant from O_2 to O when N_2 was present [20].

Analogous results have been obtained at 10 Torr in O_2/15% N_2 plasmas at temperatures between 400° and 700°C [17], although the oxidation rate was higher (21 nm in one hour at 700°C) than that reported in Reference [20]. The difference may be related to the higher N_2 content of the plasma atmosphere, which could generate higher concentrations of NO, although no measurements of NO concentration were performed. Alternatively, the electron concentration and hence the oxygen atom density may increase with N_2 addition, thereby enhancing the oxidation rate.

Substantially higher oxidation rates have been reported for 75%O_2/23.5%Ar/1.5%H_2 at 10 Torr; 41 nm of oxide was grown at 700°C in one hour [17]. This observation was ascribed to the formation of OH in the plasma atmosphere, which should be an extremely active oxidant. However, the authors stated that a higher oxygen atom concentration was also a possible reason for this enhancement. Electrical properties improved relative to oxides grown in O_2/N_2; after a forming-gas anneal at 450°C, the oxide charge and interface trap levels were ~6 x 10^{11}/cm^2 and ~4 x 10^{11}/cm^2/eV, respectively, and the MBDF was ~11 MV/cm. These improvements in interfacial properties when hydrogen and oxygen were present in the plasma atmosphere were believed to be a result of the saturation of broken bonds at the Si-SiO_2 interface by H and OH radicals [17].

The above results suggest that in plasma afterglows, at a (relatively high) pressure of ~1 Torr or above, the oxidation process depends on the presence of oxygen atoms, which can easily break Si-Si bonds at the Si-SiO_2 interface; oxidation is therefore not controlled by reaction-rate limitations at the interface. However, oxygen atoms must diffuse through the growing oxide layer; thus, when large concentrations of O are present, (parabolic) oxide growth rates are higher owing to the higher diffusion flux of O compared to O_2 through the oxide layer. In the O_2/N_2 oxidation, no

mention is made of nitrogen incorporation at the Si-SiO_2 interface. Indeed, nitrogen may not be incorporated, because of the excess O_2 (95%) present in the inlet flow. Under these conditions, Si-N bonds will probably be oxidized to Si-O; this is discussed in more detail in the section on plasma nitridation.

With regard to the above discussion, an alternative mechanism of afterglow oxidation can be considered. During the initial oxide growth phase (<35 nm of oxide), estimates of the oxidation yield of O and O^- reactions with silicon in microwave O_2 afterglows suggested that the role of O was negligible compared to O^- [22]. From observed oxidation rates, the authors proposed that O atoms recombine rapidly in the growing oxide film, and that the formation of O^- occurs at the surface of the oxide film where electrons react with O [22]. This mechanism was believed to be more important than gas-phase attachment reactions to form O^-. In this analysis, oxidation yields were calculated from anodization experiments where O^- was assumed to be the oxidizing species.

• *Inductively coupled rf plasmas*
Radio-frequency (rf) oxidation/anodization has been carried out at frequencies between 400 kHz and 13.56 MHz. Early studies of the anodization of silicon were performed at low temperatures (<250°C) and pressures (~30 mTorr) in inductively coupled 1-MHz oxygen plasmas with dc wafer bias [23, 24]. As current densities increased from 5.5 mA/cm^2 to 28 mA/cm^2, oxidation rates varied from 0.7 nm/min to 4.2 nm/min. For as-grown films, the fixed oxide charge levels were >1 x 10^{12}/cm^2. A 450°C post-metallization treatment in N_2 resulted in MBDF values near 10 MV/cm, and fixed oxide charge levels near those of thermal oxides, e.g., ~10^{11}/cm^2 for (111)-oriented silicon.

Anodization and selective anodization (using Al_2O_3 layers as a mask) of silicon were performed at 30 mA/cm^2, 600°C, and 0.2 Torr O_2 at 420 kHz [25]. Under these conditions, a film of 1 μm thickness was grown in about one hour. An increase in current density increased the growth rate further; however, at 200 mA/cm^2, extensive sputtering of the cathode material was observed. In an attempt to elucidate the anodization mechanism [25], ^{18}O oxidation experiments were used. Although anodization clearly proceeded by ion transport, it was impossible to determine whether oxygen ions or silicon ions were the primary species transported. Infrared spectra of the plasma-grown oxides were identical to those of thermally grown oxides; breakdown fields for the plasma-grown oxides were as high as 7 x 10^6 V/cm. Interface state densities of as-grown oxides were ~10^{12}/cm^2/eV; after a forming-gas anneal at 450°C for one hour, this value dropped to ~10^{10}/cm^2/eV. These results were consistent with defect centers in these layers as detected by electron spin resonance [25]. The roughness of the Si-SiO_2 interface appeared to be equivalent to that of thermally grown oxides, despite the high current densities used.

Silicon dioxide films grown at low current densities (0.5-2.5 mA/cm^2), at a temperature of 500°C, in a 13.56-MHz O_2 plasma [26], displayed electrical properties similar to those of films formed at higher current densities but lower temperatures [23, 24]. Growth rates were lower at the low current densities: ~0.33 to 1.2 nm/min for pressures between 100 and 5 mTorr, respectively [26]. Still lower

growth rates were observed when plasma oxidation (no external bias) was performed at ~15 mTorr O_2 on an unheated (except for plasma heating) silicon substrate: oxide thicknesses between 0.8 and 1.2 nm were grown in one hour, depending upon the rf power level [27]. The growth rate correlated with O_2^+ density, as determined by optical emission, during the initial growth phase (~1 nm); subsequently, transport of oxidizing species through the oxide appeared to control growth [27]. No electrical properties were reported for these films.

Silicon oxidation rates in rf reactors at low pressure and low current (plasma) densities bear much similarity to those observed in microwave downstream oxygen plasma oxidation or anodization at high pressures. Although the concentration of oxidant is reduced in low-pressure systems, the plasma emits high-energy photons and can form highly reactive radicals (e.g., O^1D), which enhance oxidation rates [28]. Of course, such mechanisms can account only for the growth of thin layers (<2-3 nm at temperatures below 400°C); further increases in oxide thickness require enhanced transport of oxidant through the oxide layer.

Addition of Cl_2 to O_2 plasmas has been reported during rf (420-kHz) plasma anodization of silicon [29]. Although the substrates were not intentionally heated, the high current density (25 mA/cm^2) led to a surface temperature of ~500°C. With the addition of 1.5% Cl_2, the growth rate was >13 nm/min, which was an increase of nearly 30% over that for pure O_2. Interface trap densities were 5 x 10^{11}/cm^2/eV; an 800°C anneal in argon reduced this value by a factor of ~7. Compared to pure O_2-grown oxides, the breakdown field distribution narrowed significantly for the 1.5% Cl_2 oxides, with an MBDF of ~8 MV/cm. Concentrations of Cl_2 above 1.5% resulted in higher interface trap densities; at 3% or greater, both SiO_2 and the silicon surface were attacked.

The throughput of substrates in plasma anodization has typically been low, since each wafer requires an electrode for biasing purposes. Several approaches have been investigated to increase the throughput while maintaining high oxidation rates; these generally use internal electrodes in a stacked arrangement [6]. An alternate approach for multiwafer processing that has demonstrated high oxidation rates with the substrates at floating potential (no external bias) is shown in **Figure 3** [30, 31]. Initial studies [30] were performed at low oxygen pressure (2-100 mTorr), frequencies in the range of 0.5-8 MHz, and temperatures between 600° and 900°C. Oxide growth at pressures below 10 mTorr appeared to be due to quartz sputtered from the reactor walls rather than oxidation of the silicon substrate; plasma oxidation occurred at pressures above 10 mTorr [30]. Interestingly, oxidation rates were highest on the side of the wafer facing away from the discharge.

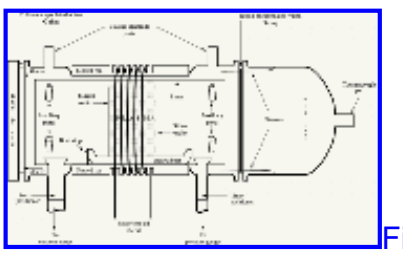
Figure 3

Subsequent investigations used rf frequencies between 6 and 21 MHz, total pressures between 85 and 500 mTorr, O_2 in Ar concentrations from 1 to 100% O_2, and rf power levels from 100 to 500 W [31]. Grid (adjacent to the wafers) biasing and silicon marker experiments during oxidation led the authors to conclude [31] that positive oxygen ions were the primary gas-phase oxidant species (i.e., cathodization of silicon was occurring) and that growth proceeded by diffusion of oxygen to the silicon surface. Cathodization kinetics obeyed a power law expression. Oxidation rate varied with rf frequency (highest rate at 10.67 MHz), with the percentage of O_2 in Ar (highest rate at 15% O_2), and with total pressure (highest rate at 85 mTorr). Rf power had the most significant effect on the oxidation rate, with essentially a linear increase of 0.4 nm/W for a two-hour oxidation. Presumably, this dependence resulted from the enhanced concentration of oxygen ions formed in the plasma at high power levels, since the oxidation rate displayed a weak dependence on temperature; E_a = 0.16 eV [30]. Oxidation rates were significant: 140 nm in two hours at 10.67 MHz, 100 mTorr, 400 W, and pure O_2; under these conditions, the wafer temperature reached ~400°C. As-grown oxides had buffered HF etch rates equivalent to those of 950°C thermally grown oxides. However, after polysilicon deposition to form capacitors, the MBDF of the oxides was ~2 MV/cm [31]. Post-oxidation anneals in O_2 at 1000°C for 15 min increased the MBDF to ~8 MV/cm.

• *Capacitively coupled rf plasmas*

A parallel-plate plasma reactor operating at 13.56 MHz was used to anodize silicon in various O_2/Ar mixtures at 475°C and current densities <1 mA/cm^2 [32, 33]. Under most conditions investigated, the growth rates were ~0.7 nm/min; at pressures below ~80 mTorr, the authors believed that oxide growth and sputter deposition (from quartz coverings in the reactor) occurred simultaneously. Oxide quality depended primarily on the use of an optimum current density, although other parameters (O_2/Ar ratio, pressure, power density) also affected oxide properties. The best oxide properties in this reactor configuration [33] at 475°C were achieved at O_2/Ar = 1.0, 40 mTorr, 1.0 W/cm^2, and 0.33 mA/cm^2; under these conditions, Q_{ox} < 1 x 10^{11}/cm^2, N_{it} < 2 x 10^{11}/cm^2/eV, and MBDF > 13 MV/cm. These oxides displayed interface states at 0.3 eV above the silicon valence band edge which seem to be due to silicon "dangling bonds." A brief rapid thermal anneal in Ar at temperatures between 800° and 1100°C, or an increase in the flux of oxidizing species to the Si-SiO_2 interface (via an increase in current density) reduced the interface state density.

A dual-frequency parallel-plate reactor with a magnetically enhanced upper electrode operating at 100 MHz and a lower (substrate) electrode operating at 41 MHz has been used to oxidize silicon at temperatures between 100° and 450°C with 2.6% O2 in argon [34]. The power supplied to the lower electrode (2 W) established low energy (~15 eV) argon ion bombardment in order to "assist" the low-temperature oxidation. Up to a thickness of ~5 nm (10 min) at 450°C, the rate appeared to be controlled by a combination of interface reaction and parabolic growth, with an effective activation energy of 0.025 eV; above 5 nm, a Cabrera-Mott model was invoked. The MBDF was ~10 MV/cm, which was nearly equivalent to that of 1000°C thermally grown oxides. Although this plasma configuration and operation was to "assist" low-temperature oxidation, anodization of silicon was likely occurring under low-current-density conditions in these studies. Indeed, the enhancements observed

and effective activation energies reported here are similar to those reported for microwave plasma anodization [15]. Furthermore, analogous results have been obtained for anodization by high-density discharges (see below).

• *Discharges sustained by dc*

Dc discharges represent a simple method of anodically or cathodically enhancing the oxidation rate of silicon [4, 5]. Unfortunately, in such configurations, contamination of the oxides due to sputtering of chamber and electrode materials can occur. The particle energy can be reduced if use is made of magnetic confinement of hot cathode discharges, although the cathode is attacked by oxygen in this type of arrangement [4, 5]. More recently, corona discharges have been investigated for plasma anodization [35-37]. In the "point-to-plane" configuration (**Figure 4**), a negative or positive dc potential is applied to a needle electrode spaced less than a few centimeters from the sample. High oxidation rates at pressures near atmospheric pressure can be achieved at reasonably low temperatures because of the high plasma density in the vicinity of the needle electrode and the drift of ions to the substrate surface. However, the nonuniform ion flux profile at the wafer surface results in a nonuniform oxide thickness across the wafer.

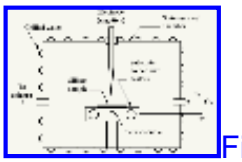
Figure 4

The use of a 50-V negative potential on a needle located 0.5 cm from the surface of a silicon wafer heated above 600°C resulted in an enhancement of oxidation rates in 1 atm. O_2 compared to thermal oxidation [35]. For example, at 900°C and 5 μA current for one hour, 100 nm of oxide was grown directly under the needle; this can be compared to ~30 nm for thermal oxidation. The enhancement was linearly proportional to the product of the local ion beam current density and the oxidation time. At a lateral distance >0.5 cm from the needle center projection on the wafer, the oxide thickness was essentially that obtained with a thermal oxidation process of equal time. With a positive needle potential [34], less enhancement occurred than in the thermal oxidation case; the thickest oxide (~70% thicker than thermal) was observed at a lateral distance of ~1 cm from the needle center. Although the transport of oxygen ions (probably O^-) is an important factor in explaining the "needle negative" results, an explanation for the results observed with the needle positive is currently lacking [35].

At conditions of 580 Torr O_2, 13 kV, a beam current of 17 μA, a needle- to-wafer spacing of 2 cm, and an unheated substrate, an oxide of 7.5 nm was grown in one hour [37]. Owing to the high current density, wafer heating probably occurred, although an estimate of the substrate temperature was not reported. Thickness uniformity was estimated to be within ±20% across a 2.5-cm-diameter wafer. It was proposed that the uniformity could be improved if an array of needle electrodes was used [37]. Interface state densities ranged from 1 x 10^{10} to 1 x $10^{13}/cm^2/eV$, with a value of 2 x $10^{10}/cm^2/eV$ at 0.17 eV above the valence band edge.

• *Nano-oxidation of silicon*

Most recently, nanostructures have been formed by the oxidation of silicon using an approach based on scanning tunneling microscopy (STM) or atomic force microscopy (AFM) [38-43]. Use was made of a conductive probe tip to establish an electric field between the tip and a surface to permit oxidation and/or anodization of silicon (or other material). Oxide film growth occurred at room temperature; thus, field-aided diffusion of anions, formed by electron tunneling from the silicon onto adsorbed surface oxygen (probably OH) species, seemed to account for growth [39, 40], although the initial studies [38] used a positively biased probe tip. With tip biases of about -7 V, oxides ~8 nm thick were grown [40]. Currents from probe tip to the surface were estimated to be <1 pA [42], while electric fields for growth were >1 x 107 V/cm [40, 43]. Since the oxidation process appeared to depend, in part, on the presence of surface water (OH groups), the widths of the oxide patterns formed were dependent on humidity in the oxidation ambient [43]. The effective activation energy of this process was estimated to be ~0.15 eV [42], which is similar to that reported for plasma-assisted oxidation, thereby confirming the importance of ionic species transport during STM or AFM growth.

• *High-density discharges*

Owing to the higher electron concentration (up to $10^{12}/cm^3$) at low pressure (0.1-50 mTorr) and low ion energies (20-40 eV), high-density discharges have been utilized to oxidize silicon. This approach permits high oxidation rates at low substrate temperature with relatively low damage. The most extensively studied configuration is the electron cyclotron resonance (ECR) reactor, depicted schematically in **Figure 5** [44]. Initial studies were performed under floating potential conditions at 0.2 mTorr O_2 [45-47]. Oxidation-rate data were not consistent with either the Deal-Grove (linear-parabolic) model [48] or a power- law model, but were analyzed according to the kinetic model proposed by Cabrera and Mott [49]. Growth occurring at the Si-SiO_2 interface was indicated by ^{18}O marker studies. A small amount of exchange of ^{18}O with the SiO_2 lattice took place during oxidant transport, suggesting that the oxidant formed under plasma conditions was more reactive than the primary reactant in dry thermal oxidation, where no exchange was observed. Growth rates were low (10 nm in one hour at 350°C), consistent with substrate floating conditions. Infrared spectra were identical to those of thermal oxides, but HF etch rates were 1.1 to 1.5 times those of thermal oxides. No electrical properties of the oxides were reported.

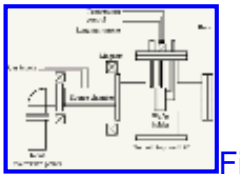
Figure 5

A distributed ECR system has been used to oxidize silicon substrates under constant-voltage conditions [50]. Although the temperature was not controlled, substrate temperature was estimated to be ~200°C. Typical oxide growth in O_2 was ~70 nm in two hours at a pressure of 3 mTorr. The oxidation rate was a function of wafer position with respect to the plasma stream, approximately tracking the ion density and estimated wafer temperature. As-grown oxide properties were not

reported. However, after a gate metallization anneal, the MOS capacitors had fixed oxide charge levels of 5 x 10^{11}/cm^2, interface trap densities of 5 x 10^{11}/cm^2/eV, and mobile ionic charge densities of 7 x 10^{10}/cm^2. The MBDF was 7.8 MV/cm.

Oxidation of silicon under floating or dc bias conditions at pressures between 0.03 and 10 mTorr and substrate temperatures between 250° and 450°C have been performed using an O_2 ECR discharge [44, 51]. Oxidation- rate data as a function of microwave power, substrate temperature, 1 mTorr pressure, and with the substrate unbiased, but with a high resistance path to ground (through the thermocouple connection) are shown in **Figure 6** [44]. Oxidation rates were significantly higher than those for thermal oxidation; a 1000°C atmospheric pressure O_2 oxidation displayed a rate similar to that of the 723 K oxidation shown in Figure 6. At microwave powers below ~500 W, the effective activation energy for oxidation was 0.06-0.1 eV, while above 700 W, the effective activation energy was zero. However, even when the discharge was sustained with 700 W of microwave power, silicon substrate heating by the plasma flux was low, so that the plasma- enhanced oxidation rate was clearly not due to a thermal oxidation mechanism. Indeed, rate data showed a better fit to an ion space-charge-limited growth model [52] than to a linear-parabolic model [48]. Under the conditions studied, no difference in rates was observed for ECR oxidation of p- versus n-type silicon. However, (111)-oriented silicon showed an ~10% increase in rate compared to that of (100); this difference was higher than the standard deviation of the oxidation runs (~3%). At present, the reason for such differences is unknown.

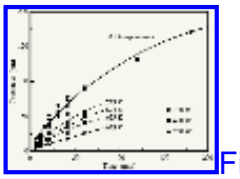
Figure 6

ECR oxides grown under substrate floating and grounded conditions had chemical and electrical properties similar to those of thermally grown oxides, provided the oxide thickness was less than 30 nm [44, 51]. Thicker oxides had buffered oxide etch (BOE) rates between 1.5 and 3.0 times those of oxides thermally grown in O_2 at 900°C. Such results may be due to the radiation exposure and total current that flowed during the growth process. Under cathodic bias (substrate holder negative), oxidation rates were similar to those obtained under floating potential [51, 53]. However, the refractive index, BOE etch rate, and MBDF indicated that these oxides had higher defect levels than thermally grown oxides, and thus were unacceptable for device fabrication [51].

ECR oxides with the best thickness uniformity and the best physical and electrical characteristics have been grown under anodic (substrate positive) bias. Anodizations performed under constant-current and constant-voltage conditions yielded identical oxide properties [51]. Transmission electron microscope studies indicated that the Si-SiO_2 interface was as smooth and uniform as that observed in thermally grown Si-SiO_2 systems, with a transition region from crystalline silicon to the amorphous oxide of 1-1.5 nm [51].

Constant-current anodization (20 mA/cm^2) displayed three growth regimes, as shown in **Figure 7** [51] : an initial region (<10 nm) that appeared to be dominated by concentration gradients, a linear growth regime from ~10 nm to 100 nm (ohmic behavior), and a region greater than 100 nm, where space-charge effects dominated. The rate coefficient values in the linear (ohmic) regime (2.45 nm/min at 1 mTorr O_2) are similar to those reported for rf plasma oxidation at equivalent current densities [24]. Current efficiencies were approximately 1 x 10^{-3} [51] ; these values are analogous to those reported for similar current densities in rf and microwave plasma oxidation [15, 23]. Furthermore, the overall oxide conductivity calculated from constant-current anodization data [51] was ~4 x 10^{-9} Ω^{-1}-cm^{-1}, which is equal to that measured for thermally grown SiO_2 [54]. Finally, previous studies have also ascribed nonlinear growth kinetics during constant-current anodization to space-charge limitations [4, 13].

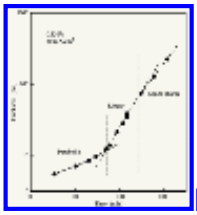
Figure 7

Constant-voltage anodization, performed at low bias voltage (+5 V), where no alteration of plasma characteristics was observed due to the applied bias, obeyed a space-charge-limited ionic transport model [51]. Current efficiencies for constant-voltage anodization were slightly lower than those observed for constant-current anodization [51]. Constant-voltage anodization studies extending to high bias (up to +60 V) used a Cabrera-Mott model for charged-particle transport to describe the kinetics [53, 55]. Since the area for current flow was not defined for the high-bias conditions, it is difficult to compare and contrast the results of these two studies.

Growth of thin oxides (up to ~9 nm) by ECR constant- voltage anodization at +30 V, with an undefined area for current flow and a temperature established by the anodization process, yielded oxides with slightly different Si-O bonding structures than those observed for thermally grown oxides, as determined by Si_{2p} XPS spectra [56]. These results were attributed to the lower-temperature interface formed in plasma growth. In addition, no significant differences in plasma anodization rate among (111), (110), and (100) were observed [56].

The high growth rates under anodic conditions, compared to those of thermal oxidation at equivalent temperatures, are believed to be due to the transport of O^- across the growing oxide layer by the applied field [51, 53]. Under low-pressure conditions and modest (>10 V) sheath potentials, it is unlikely that negatively charged oxygen species in the plasma have sufficient energy to reach the substrate. Therefore, atomic oxygen from the plasma probably adsorbs onto the oxide surface and forms O^- via plasma electron attachment, as suggested previously for downstream plasma oxidation [4]. A simple reaction mechanism can then be proposed to describe the oxidation kinetics by considering adsorption of O onto a surface site S_{ad} [51]:

$$O(g) + S_{ad} \leftrightarrow O_{ad}, \quad (1)$$

$$O_{ad} + e^- \longrightarrow O^-, \quad (2)$$

$$2\,O_{ad} \longrightarrow O_2\,(g). \quad (3)$$

This kinetic scheme predicts that the oxidation rate is proportional to the square root of the gas-phase oxygen atom concentration; indeed, this dependence has been confirmed experimentally [51].

As-grown ECR oxides (20-30 nm thick) displayed significant fixed oxide charge (>1 x $10^{11}/cm^2$) and a high interface trap density (>1 x $10^{12}/cm^2/eV$) compared to thermal oxide control samples; no mobile charge was detected in any of the samples [51]. Such values are similar to those reported for other ECR-grown oxides [50]. The charge levels observed were likely due to UV and electron flux from the plasma. Breakdown fields were ~4, ~8, and ~11 MV/cm for floating, anodic, and thermal oxides, respectively, for aluminum-metallized devices [51]. When polycrystalline silicon was used as the gate electrode, the effect of plasma-induced radiation damage was reduced [51]. Since the anneal step following polysilicon deposition was performed at 850°C in nitrogen, the fixed charge and interface trap density dropped to those of a thermal oxide (4.7 x $10^{10}/cm^2$ and 1 x $10^{11}/cm^2/eV$). Intrinsic breakdown fields also improved with the polysilicon process, yielding MBDF of 10-12 MV/cm. However, a slight low-field leakage current was noted for these samples, probably a result of residual oxide damage [51]. This observation is consistent with reports of interfacial damage due to ECR oxidation [57]. Furthermore, it has been suggested that this interfacial damage (structural disorder) may account for the general observation that little, if any, orientation dependence is observed for plasma-assisted oxidation [7], although specific results will depend upon the growth temperature, ion and photon flux and energies, and the current density used during anodization.

A helical resonator plasma system, operating under moderate plasma density (up to 4 x 10^{10} electrons/cm^3) has been used to form thin SiO_2 films on silicon [58]. Anodization rates at 350°C, 30 mTorr O_2, and a defined anodic current of 3.8 mA/cm^2 were described well by both parabolic and power-law expressions, probably owing to the relatively low current densities used. The low current density in this system compared to that used in ECR reactors also resulted in lower oxidation rates (23 nm was grown in one hour). However, these rates were substantially higher than those achieved by thermal oxidation at such temperatures. For 20-nm oxides grown on p-type (100) silicon and aluminum metallization followed by a forming-gas anneal at 400°C, the fixed oxide charge was ~2 x $10^{11}/cm^2$ and the MBDF was 5.3 MV/cm. Such values are similar to those obtained from ECR-grown oxides with analogous post-anodization processing [44].

Before leaving the topic of plasma-assisted oxidation/anodization of crystalline silicon, a further remark should be made concerning the mechanism(s) involved in oxide growth. Clearly, O atoms are key reactants in oxidation systems, and O^- appears to be critical during anodization. However, another gas-phase species that may play an important role is ozone (O_3). Oxidation of silicon at 550°C in O_2 containing 3-4% by volume O_3 [59] yielded oxide films of 14 nm in one hour; oxide

thicknesses under identical conditions using only O_2 gave oxide thicknesses <2 nm [59]. The oxidation rates, measured between 400° and 550°C, obeyed a parabolic rate expression, with an effective activation energy of 0.8 eV. This value is less than that for diffusion of O_2 through SiO_2 (>1.2 eV). The authors suggested that oxidation occurred in O_3 by dissociation of O_3 on the surface of SiO_2, to give O_2 and O. The O diffused rapidly, compared to O_2, to the Si/SiO_2 interface, and thus was the primary oxidant [59]. Clearly such mechanisms are likely in plasma environments, although the concentration of O_3 may be much less than that used in Reference [59].

Plasma oxidation and anodization of SiGe

Silicon-germanium single-crystal layers have been oxidized by rf and ECR O_2 plasmas. No germanium pile-up occurred at the oxide-SiGe interface with either plasma process. With 13.56 MHz rf, 10% Ge/Si MBE layers were anodized at ~80°C, 0.15 Torr, and +50 V [60, 61]. Fifteen minutes of anodization yielded ~50 nm of oxide, which was equal to that grown on pure silicon. After Al metallization and a post-metallization anneal in forming gas, the fixed oxide charge on SiGe was ~1 x $10^{12}/cm^2$ and the mid-gap interface state density was ~1.6 x $10^{12}/cm^2/eV$. ECR anodization of 20% Ge/Si MBE layers was performed in 0.5 mTorr O_2 at voltages up to +14 V and temperatures up to 500°C [62, 63]. Approximately 4 nm of oxide could be grown at +10 V in one hour at 300°C (apparently, current densities in this study were relatively low). MOS capacitors with aluminum metallization were used to evaluate electrical properties of these oxides. The best electrical results were obtained when a pre-anodization hydrogen plasma was used to remove the native oxide from the SiGe surface. Pre-cleaned 10-nm oxides grown at 400°C and annealed in vacuum at 450°C yielded oxides with a fixed charge of ~-1.5 x $10^{11}/cm^2$ and a mid-gap interface state density of ~8 x $10^{11}/cm^2/eV$. Although the authors have not observed Ge pile-up at the oxide-SiGe interface by Auger electron spectroscopy, the negative fixed charge reported for these films suggests that excess Ge may be present.

Plasma oxidation and anodization of amorphous and polycrystalline silicon

Owing to the relatively high growth rates of plasma-enhanced oxidation and anodization of crystalline silicon at low temperatures, significant interest has arisen in the low-temperature growth of oxide layers on amorphous and polycrystalline silicon. Specifically, growth temperatures below 450°C are compatible with thin-film transistor (TFT) fabrication on glass substrates, and silicon structural/bonding properties may remain unaltered. In addition, Si/SiO_2 interface properties resulting from plasma growth may be improved compared to those obtained with deposited SiO_2.

• *Amorphous silicon*

Plasma-deposited amorphous silicon (a-Si) films were oxidized (to an unspecified thickness) at 250°C in a parallel-plate plasma reactor in N_2O for 30 minutes [64]. Compared to the other methods of surface passivation studied, which included 10-nm deposits of silicon carbide, silicon oxide, and silicon nitride, the plasma-grown oxide was superior, as evidenced from the reduction in interface state density.

Furthermore, the surface passivation achieved with the N_2O plasma was equivalent to that obtained with chemical (nitric acid) passivation. In this study, no mention is made of the possibility of nitrogen incorporation from N_2O at the Si/SiO_2 interface or at other defect sites in the a-Si film.

Plasma-deposited a-Si films were oxidized (to an unspecified thickness) at 270°C and ~0.7 Torr O_2 in a parallel-plate plasma reactor for 150 minutes [65]. The bulk a-Si was not altered by this process; only surface oxidation took place to close some of the micropores present.

Sputtered a-Si films deposited onto thermally oxidized silicon wafers were oxidized under substrate floating conditions in a 13.25-MHz helical resonator plasma reactor at temperatures between 300° and 400°C, 3.8 mA/cm^2, and 30 mTorr O_2 [66]. Little change in oxide thickness was observed over the temperature range studied; in general, the oxidation rate was ~50% larger for a-Si than for crystalline silicon under the same conditions. A power law rate expression described well the rate data for a-Si oxidation. Because of the floating substrate conditions, the oxide thickness increased very slowly after a thickness of 12 nm (20 min at 300°C) was achieved; an additional 1 nm of oxide required an additional 20 minutes of oxidation.

TFTs have been fabricated by oxidizing low-pressure chemically vapor-deposited (LPCVD) a-Si using an O_2 ECR plasma (under unspecified conditions) to form a 40-nm gate oxide [67]. Crystallization of this oxidized a-Si layer yielded an Si/SiO_2 interface with average roughness <0.3 nm, essentially the roughness of as-deposited a-Si. This is a significant improvement over that observed with ECR oxidation after a-Si crystallization, where the average interface roughness was ~0.8 nm [67]. The current-voltage characteristics of the TFTs with a-Si oxidized before crystallization and a-Si oxidized after crystallization were similar. However, unlike the TFTs formed by oxidation after crystallization, those TFTs fabricated by oxidation prior to crystallization showed no appreciable degradation of mobility with gate-voltage increase [67].

• *Polycrystalline silicon*

ECR oxidation of recrystallized polycrystalline silicon has been used to form a gate insulator for TFTs. Oxidation was performed for two hours at 400°C in an O_2/20% Ar atmosphere under substrate floating conditions to grow a 42-nm oxide [68, 69]. The roughness of the plasma-oxidized surface [68] was only slightly greater than that of the unoxidized polycrystalline surface (0.7 versus 0.48 nm), but considerably less than the roughness of the thermally oxidized surface (1.7 nm for a 950°C oxidation). This reduction in roughness was ascribed to the field-enhanced nature of the ECR oxidation, so that asperities at the polycrystalline silicon surface oxidize faster than the surrounding material [68]. In addition, electron spin resonance studies demonstrated "dangling bond" passivation by the ECR oxidation [69]. Finally, the interface state density of ECR-grown oxides was lower than that of either a 470°C LPCVD oxide or a thermally grown oxide [69]. These factors contributed to the improved capacitor MBDF (>5 MV/cm) compared to that of either LPCVD or thermally grown oxides (<5 MV/cm). TFTs fabricated without plasma hydrogenation but using ECR oxidation for gate formation exhibited field-effect mobilities of 60 and 80 $cm^2/V\text{-}s$ for n-channel devices when SiH_4 and Si_2H_6 were used for polycrystalline

silicon deposition, respectively, and 48 and 69 cm^2/V-s for p-channel devices where deposition of polycrystalline silicon was performed using SiH_4 and Si_2H_6, respectively [68]. These results were ascribed to the smoother interfaces obtained with plasma oxidation, stable passivation of dangling bonds, and plasma cleaning during oxide growth [68, 69].

TFTs have also been fabricated using a two-step gate-oxide growth process. The use of helical resonator O_2 oxidation at 300°C to form a 10-nm oxide followed by the plasma-enhanced CVD of a 15-nm SiO_2 film at 350°C resulted in a gate-oxide stack that gave a polycrystalline silicon n-channel TFT mobility of 31 cm^2/V-s [66]. Similarly, ECR oxide growth at 400°C to a thickness of 30 nm, followed by atmospheric pressure CVD at 370°C of a 70-nm SiO_2 film yielded a gate-oxide stack that gave a polycrystalline silicon n-channel subthreshold swing of 1.58 V/decade and a gate-oxide breakdown field of >9 MV/cm [70]. These results are consistent with previous studies that have reported improved plasma-grown oxide characteristics on crystalline silicon by low-deposition-rate formation of a thin plasma-grown oxide, followed by PECVD of a thicker SiO_2 layer to complete the stack. For instance, improved-quality Si/SiO_2 interfaces have been formed by growing a 3-4-nm oxide in a parallel-plate reactor at 350°C and high pressure (~1 Torr), followed by a PECVD oxide deposition [71] or by a downstream oxygen atom oxidation to form ~0.5 nm of oxide, followed by a downstream or remote deposition of SiO_2 [72].

Plasma nitridation and oxynitridation of single- crystal silicon

Relative to plasma-assisted oxidation of silicon, few studies of plasma nitridation of silicon have been published. Direct growth of nitride layers onto silicon has proven difficult for two primary reasons. Silicon surfaces exposed to air have native oxide coatings; also, silicon reacts rapidly with oxygen atoms or water vapor. As a result, both nitride and oxide bonding structures are generally formed during plasma growth processes that either expose (native-oxide-covered) silicon surfaces to nitrogen atoms or expose *in-situ*-cleaned silicon surfaces to nitrogen atoms in the presence of oxygen atoms, oxygen molecules, or water vapor (intentional or unintentional). Most recent studies have investigated oxidation or anodization of silicon in nitrous oxide (N_2O) plasmas. In this case, nitridation occurs at the silicon surface, and sometimes at the growing SiO_2 surface, while oxynitrides may form in the bulk oxide.

• *Nitridation in NH_3, N_2, and N_2/H_2 mixtures*

Because of the high density of silicon nitride layers, high temperatures (>800°C) have been needed to grow thin films (>50 nm) in several hours using rf frequencies. For instance, an ~50-nm film was grown using an Ar plasma with small (2-8%) additions of N_2, NH_3, or N_2/H_2 in an rf (400-kHz) induction system at a pressure of 80 mTorr and temperatures below 850°C [73]. With capacitively coupled systems at 13.56 MHz, the silicon wafer in contact with the rf-driven electrode, 950°C, and a pressure of 1 Torr, an NH_3 plasma grew 5.5 nm in one hour [74], while an N_2/H_2 plasma at 900°C and the same conditions grew 9 nm in one hour [75, 76]. Direct comparison of the results of these studies is difficult, since the potentials in the capacitively coupled systems were clearly different. All films had oxygen contamination ranging from ~2% [74] to 10-15% [73, 75, 76] ; the origin of the

oxygen was presumed to be reactor leaks and native oxide layers. By analogy with silicon anodization, the nitridation mechanism was believed to be the incorporation of nitrogen species into the growing nitride surface, followed by diffusion of the nitrogen species (probably charged as well as uncharged) to the Si/SiN_x interface [74-76]. The growth rate obeyed a parabolic rate expression, with an effective activation energy, when an anodizing voltage of -150 V was applied to the substrate electrode, of 0.25 eV [76]. The presence of hydrogen appeared to enhance the diffusion or drift of nitrogen species [76]. MBDF for as-grown nitride layers was ~3 MV/cm [75].

In an attempt to eliminate oxygen contamination during film growth, nitride layers were grown on silicon in an ultrahigh-vacuum chamber after Ar sputter-removal of the native oxide layer [77]. The plasma growth atmosphere was 5% NH_3/95% N_2, 375 mTorr, and 13.56 MHz, with the silicon substrate at ~400°C; no anodization voltage was applied. According to XPS estimates, the nitride thickness saturated after ~1 min of nitridation at ~4.5 nm. The nitride appeared to be nonstoichiometric, with a deficit of N atoms; the authors believed that the layer was a two-phase mixture of Si_3N_4 and Si. Apparently, no oxygen was detected in the nitride layer. However, evidence for the existence of N-H bonds was obtained from XPS data.

Similar to nano-oxidation of silicon, nano-nitridation of silicon has been reported recently, using an AFM with a negatively biased silicon tip [78]. This study investigated silicon nitride growth in 50 Torr of either N_2 or NH_3; only NH_3 generated a nitride layer (~250 nm), presumably owing to the lower bond-dissociation energy of $H\text{-}NH_2$ compared to that of the nitrogen triple bond. Analogous to nano-oxidation, silicon nano-nitridation is believed to be controlled by the electric field (tip negative) established between the AFM tip and the silicon, since negative biasing of the silicon substrate gives irreproducible results [78].

• *Nitridation and oxynitridation in N_2O and N_2/O_2 mixtures*

Downstream microwave discharges have been used to grow silicon oxynitride layers using N_2O at 3 Torr with a substrate temperature of 600°C [79] and using N_2/O_2 mixtures at 1 Torr with a substrate temperature of 550°C [80]. With N_2O, nitrogen was incorporated throughout the 7-8-nm oxide layer, but the concentration was highest at the SiO_2 surface and decreased to the Si/SiO_2 interface [79]. This distribution is similar to that observed in oxides thermally (furnace) nitrided with NH_3. Nitrogen in the bulk oxide gave high tunneling currents, but MBDF ~8 MV/cm; the effective charge density was ~3 x $10^{11}/cm^2$, while the interface state density was >2 x $10^{12}/cm^2/eV$ [79]. These results are consistent with low N concentrations at the Si/SiO_2 interface, as observed by SIMS analysis. With N_2/O_2 mixtures, nitrogen was incorporated primarily at the Si/SiO_2 interface [80]. With a N_2/O_2 ratio of 380, the oxide thickness was ~3 nm, while with a N_2/O_2 ratio of 20, the oxide thickness was ~7 nm. Furthermore, the peak nitrogen density at the Si/SiO_2 interface was independent of oxidation time. Since upstream excitation/dissociation of N_2 did not incorporate N into an ~10-nm SiO_2 film, the author concluded that oxidation was required in order for oxynitridation to occur [80]. However, mass-spectrometric sampling near the substrate surface indicated that at least 1% N and 0.4% O, and

similar amounts of NO and N_2O, reached the sample surface [80].

The above results suggest that NO may play an important role in the plasma-assisted nitridation and oxynitridation of silicon. Indeed, nitric oxide (NO) has been suggested to be an important reactant in thermal oxidation/ nitridation of silicon in N_2O [81, 82]. In addition, upstream 13.56-MHz excitation of He/N_2O mixtures at 300 mTorr permitted growth of thin oxide layers at 300°C with nitrogen incorporation at the Si/SiO_2 interface; mass spectrometry and optical emission studies of the gas phase suggested that NO^+ and excited oxygen molecules (O_2^*) were the dominant species impinging on the oxidizing surface [83]. On the basis of these results, a mechanism that involved the insertion of NO^+ into Si-Si bonds followed by oxidation by O_2^* was proposed to account for the interface nitridation and oxide growth, respectively [83].

Using a helical resonator plasma source, growth of oxynitrides in N_2O and nitridation of SiO_2 in N_2 has been performed at temperatures below 400°C [58, 84]. Constant-current anodization of silicon at 30 mTorr N_2O, 3.8 mA/cm^2, and 350°C gave ~18 nm of oxide in one hour, and the anodization rate was described well by both power-law and parabolic growth models, indicating that growth was not self-limiting. The oxide growth rate was lower by a factor of 2-3 than that observed in O_2 plasmas under identical conditions. Reduced growth rates were due to the lower electron density in N_2O compared to O_2 plasmas, as well as an inhibition effect due to Si-N bonding at the Si/SiO_2 interface. Angle-resolved XPS indicated that nitrogen was incorporated in a $N\text{-}Si_3$ bonding configuration, primarily at the Si/SiO_2 interfacial region. The nitrogen concentration increased with anodization time, reaching ~4 atomic % (at.%) with a 15-nm oxide [84]. As the oxide thickness increased, nitrogen, previously located at the interface, moved into the oxide bulk, where oxynitride structures formed; some nitrogen recombined to form N_2, which diffused out of the oxide. A variety of oxynitride structures were observed at different binding energies, as depicted in **Figure 8** [84]. Anodized samples heat-treated in N_2 to temperatures up to 1000°C lost nitrogen, primarily in the oxynitride configuration, owing to molecular rearrangement and outdiffusion of N_2. However, even after a 1000°C heat treatment for 30 min, ~0.4% nitrogen (as $N\text{-}Si_3$) remained at the Si/SiO_2 interface [84]. This result suggested that a small amount of nitrogen is stable at the Si/SiO_2 interface even when incorporated at low (350°C) temperature. The interfacial stability of $N\text{-}Si_3$ has been ascribed to a reduction in the gradient of interfacial stress due to density differences among Si, Si_3N_4, and SiO_2 [85].

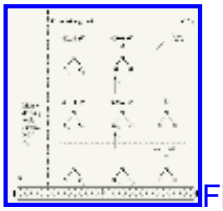
Figure 8

Residence time in the plasma reactor has also been shown to affect the nitrogen concentration in N_2O-anodized samples [86]. At temperatures up to 400°C, lower

pressures and higher N_2O flow rates yielded lower nitrogen contents in the bulk oxide layer and at the Si/SiO_2 interface (~0.5-1%). Such observations may be related to the formation and thus concentration of particular chemical moieties (e.g., NO) that can be formed in the plasma. Indeed, changes in the concentrations of NO and NO_2 have been invoked to account for differences in the amount of nitrogen incorporated in furnace-grown oxynitrides [81, 82].

Nitridation of plasma-grown SiO_2 films has been performed by application of an anodizing (silicon positive) voltage during exposure of the oxide film to a N_2 helical resonator plasma [58]. When an 8.6-nm helical-resonator-grown SiO_2 film was exposed to a N_2 plasma at 0.75 mA/cm^2 at 350°C for five minutes, the film thickness increased to 9.1 nm. Nitrogen was incorporated throughout the oxide layer (>5%) in a $N-Si_3$ configuration, although the highest concentration (~8%) was at the SiO_2 surface. When the above N_2 anodization process was applied to a 12.5-nm thermally grown (950°C in O_2) SiO_2 film, no nitrogen was detected at the Si/SiO_2 interface, but nitrogen (as $N-Si_3$) was present at the SiO_2 surface and into the bulk oxide [87]. These results suggest that current-driven nitridation proceeded from the oxide surface toward the oxide bulk, probably due to the absence of intentional oxidation species (e.g., O from O_2 or N_2O). Clearly, small concentrations of oxygen from the quartz reactor walls, quartz substrate holder covers, or background water vapor were likely present, but the absence of a measurable change in the oxide thickness after nitridation suggested the inability of these oxygen species to cause further oxidation [87]. These results are in contrast to previous studies indicating the inability to nitride thermally grown SiO_2 layers with a N_2 discharge [80]. However, in the helical resonator studies [58, 87] the nitridation process was current-driven, thereby permitting the incorporation of nitrogen without (apparent) oxidation.

Electrical properties of N_2O-grown and N_2-nitrided oxides have also been measured. After a forming-gas anneal at 400°C for 30 min, both the 350°C N_2O anodically grown oxide and the 950°C thermally grown oxide gave charge densities of ~8.7 x $10^{10}/cm^2$ [86, 87]. MBDFs were~8.5 MV/cm and ~4.1 MV/cm for the thermal oxide and the N_2O anodically grown oxide, respectively [86]. At lower pressure or higher flow rate (thus lower residence time), the nitrogen concentration decreased, while the oxide charge level and MBDF increased to ~1.5 x $10^{11}/cm^2$ and >7 MV/cm, respectively [86]. The 350°C N_2 anodized thermal oxide had a charge density and MBDF of 3.9 x $10^{11}/cm^2$ and <1 MV/cm, respectively [87]. Clearly, anodically nitrided oxides with nitrogen at the surface and in the bulk of the oxide have high leakage currents; these observations are consistent with previous studies of SiO_2 thermal nitridation with NO and NH_3 at temperatures greater than or equal to 1000°C [88, 89].

A high-density helicon N_2 plasma at 4 mTorr has been used to perform downstream surface nitridation of a 4-nm thermally grown SiO_2 layer [90]. Although the surface was not intentionally heated nor biased, a 10-s exposure at a current density of ~4 mA/cm^2 incorporated >15 at.% nitrogen into the top ~5 nm of the SiO_2 surface. Suppression of boron penetration due to this surface-nitrided layer was observed

[90, 91], indicating the possibility of altering oxide surface properties at low (probably <100°C) temperature. Furthermore, this surface nitridation did not degrade n-channel nor p-channel mobility in 0.18-μm CMOS devices compared to those observed with pure SiO_2 as the gate dielectric [91].

Plasma nitridation and oxynitridation of polycrystalline and amorphous silicon

Analogous to plasma-assisted oxidation of polycrystalline silicon in O_2, ECR oxidation (without applied bias) of polycrystalline silicon in N_2O plasmas at 400°C and 2 mTorr reduced the Si/SiO_2 interface roughness [92-94]. This fact is evident in the AFM images of heavily phosphorus- doped polycrystalline silicon surfaces (**Figure 9**), where N_2O ECR oxidation reduced the roughness compared to both unoxidized and thermally oxidized films [94]. Such results are also in agreement with thermal oxidation of polycrystalline silicon (at 900°C) in pure N_2O [95]. The improvement in surface smoothness due to ECR oxidation appeared to be related to both the low-temperature oxidation and a reduced silicon orientation dependence on growth rate in N_2O compared to O_2 oxidation [94], although it is likely that field effects at asperities also play a role, as noted previously [68]. The orientation effects observed in O_2 plasmas [94] are consistent with very low current densities (no anodization or controlled area for current flow), and thus the trends are similar [except for (110) orientation] to those of thermal oxidation. Plasma oxidation in N_2O, however, yielded a self-limiting oxide of thickness ~16 nm under the conditions described above [94]. Nitrogen incorporation at the poly-Si/SiO_2 interface was believed responsible for inhibiting diffusion of oxidant to the silicon surface [94], again in agreement with thermal oxidation/nitridation results.

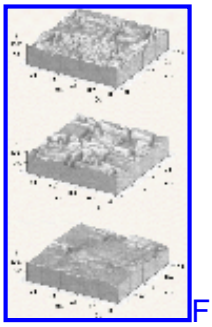
Figure 9

Capacitors fabricated from N_2O plasma-oxidized n_+ polycrystalline silicon had MBDF values of >5 MV/cm, with no difference in results for positive or negative bias [94]; this was in contrast to the results observed for thermal oxide layers on polycrystalline silicon, and was ascribed to the improved interface roughness [94]. TFTs fabricated from N_2O plasma-oxidized n_+ polycrystalline silicon displayed improved performance compared to those fabricated using thermally grown oxides. After a forming-gas anneal at 450°C, the mobilities of n-channel TFTs were 16.6 and 41.2 $cm^2/V\text{-}s$, respectively, for thermal (O_2) oxide and N_2O plasma oxide [94]. This improvement was believed to be due both to the reduced interface roughness and to the passivation effect of nitrogen at the interface [94].

Amorphous silicon has been oxidized (no applied bias) in N_2O in a parallel- plate plasma reactor at 13.56 MHz, 300°C, and ~135 mTorr [96, 97]. The oxide thickness saturated after ~20 min oxidation time at ~5 nm, which was essentially identical to the oxide grown in pure O_2. Nitrogen accumulated at the SiO_2/a-Si interface, analogous to that observed with single-crystal and polycrystalline silicon. However, at short oxidation times (~1 min), nitrogen was uniformly distributed throughout the oxide layer, while at longer times, some nitrogen appeared at the SiO_2 surface and accumulated at the SiO_2/a-Si interface [97]. Nitrogen at the SiO_2 surface was believed to be bonded to oxygen (from XPS binding energy of N_{1s}); this nitrogen was eliminated by vacuum annealing for two hours at 250°C [97]. However, owing to the large number of bond angles and bonding structures possible in N_2O plasma-oxidized a-Si, it is also likely that a silicon oxynitride configuration can account for the XPS peak observed.

Preliminary XPS studies of a-Si oxidized to a thickness of 11 nm (20 min oxidation time) at 350°C, 30 mTorr N_2O, and substrate floating conditions indicated that nitrogen was present near and at the a-Si/SiO_2 interface in a N-Si_3 bonding arrangement [87]. Nitrogen was also present in oxynitride structures in the oxide bulk [87] at XPS peak positions analogous to those observed in the N_2O oxidation of crystalline silicon [84]. In N_2O-oxidized a-Si, higher nitrogen concentrations (~1.5-2.3 at.%) were incorporated than in the N_2O oxidation of crystalline silicon (under substrate floating conditions). Such results are likely due to the higher concentrations of substoichiometric bonds in a-Si compared to crystalline silicon. Furthermore, nitrogen annealing of the a-Si structures at 500°C for 30 min resulted in a loss of nitrogen in the oxide bulk, but the interfacial region retained the 1.5-2.3 at.% nitrogen in the N-Si_3 configuration; similar results were observed for forming-gas anneals at 400°C [87]. These observations suggest that nitrogen stabilizes substoichiometric oxygen bonding structures in oxidized a-Si.

The neutral defect density for the N_2O-oxidized a-Si, as measured by ESR, was equivalent to that observed for as-deposited a-Si, and a factor of 4 less than that for O_2-plasma-oxidized a-Si [96, 97]. The lower defect density correlated with a smoother interface morphology (<2-nm undulation) compared to the O_2 plasma-oxidized sample (~3-nm undulation), which was assumed to be related to nitrogen incorporation and perhaps to lower ion bombardment energies for N_2O fragments relative to O_2^+ [96].

Porous silicon (PS) has been nitrided at 100°C using N_2 in a parallel-plate plasma reactor operating at 13.56 MHz and ~135 mTorr [98]. Nitridation occurred more rapidly on PS than it did on (111) silicon surfaces. Since the PS was exposed to air for several days prior to nitridation [98], the N_2 plasma probably formed oxynitride structures. As in a-Si, nitridation decreased the density of neutral defects in PS, as determined by ESR. Because the low-temperature nitridation process appeared to nitride silicon crystallites in the PS, control of crystallite size in PS may be possible [98].

Summary and conclusions

A variety of approaches to the plasma-assisted oxidation or anodization of silicon at low (<600°C) temperatures have been pursued over the past 30+ years; these include microwave, rf, dc, ECR, and helical resonator discharges. In all cases, significant enhancement of the oxidation rate compared to thermal oxidation at similar temperatures has been observed, offering the possibility of reduced thermal budgets for microelectronic device processing. The rate enhancements are due to both the plasma-assisted generation of reactive species and the application or generation of electric fields across the growing oxide layers. Still larger enhancements in oxidation rate have been observed when positive substrate biases (e.g., anodization) were used. In most instances, O^- is believed to be the primary oxidant during anodization in O_2, and perhaps in N_2O also, but the exact oxidation mechanism has not been established.

The use of N_2O for plasma-assisted oxidation or anodization of silicon results in the incorporation of nitrogen into the growing oxide layer, primarily at the Si/SiO_2 interface in a $N\text{-}Si_3$ bonding configuration. Despite the low temperatures used to grow such layers, a small amount (~0.5-1%) of the nitrogen incorporated is stable to high-temperature (~1000°C) annealing in N_2. Improvement in the electrical properties of devices incorporating nitrogen at the interface is typically observed. Nitrogen incorporated in the oxide bulk is not stable; anneals at temperatures above the deposition temperature appear to remove most, if not all, of the nitrogen. Nitrogen (N_2) plasmas can be used to nitride SiO_2 or silicon, although the rates are low unless a current-driven (anodization) process is used. Nevertheless, since surface nitridation of SiO_2 is possible with downstream plasma processes, the inhibition of boron diffusion is possible at low temperatures (around room temperature).

The primary limitation in the use of plasma-grown oxides in ULSI devices is control of oxide (or nitrided oxide) properties, in particular, oxide charges and MBDF. Although the use of high-density discharges has improved oxide properties considerably, post-oxidation heat treatments at temperatures above the growth temperature have been necessary to achieve good dielectric properties. Even after such heat treatments, low field leakage currents usually exist. Part of the problem appears to be oxide damage due to plasma radiation. In addition, if high current densities are used, oxide damage is promoted. One approach to partially circumvent such issues involves the growth of a thin oxide using low-power discharges (where the sample is placed either within or downstream of the discharge) followed by deposition of additional oxide by CVD or PECVD methods; unfortunately, this adds complexity to the oxide growth process, and an additional interface (dielectric/dielectric) to device structures. Nevertheless, devices with adequate electrical properties have been reported for these structures.

Results analogous to those reported for the oxidation, anodization, or nitridation of crystalline silicon have been observed for polycrystalline, amorphous, and porous silicon. Because of the low-temperature process, such film-growth methods are attractive for flat-panel display applications. Furthermore, interfaces between the plasma-grown oxides or oxynitrides and either polycrystalline or amorphous silicon are smoother than those obtained via thermal oxidation; thus, improved electronic device properties can be achieved.

Acknowledgments

The author sincerely appreciates the helpful comments and suggestions concerning this manuscript provided by Dr. Sita Kaluri and Mr. Scott Gold. Funding for the author's work in the area of plasma-assisted oxidation and nitridation has been provided most recently by The National Science Foundation under Grant No. CTS 9214138, and The Advanced Research Projects Agency under Contract No. F33615-96-1-1939.

References

Received November 26, 1997; accepted for publication April 27, 1998

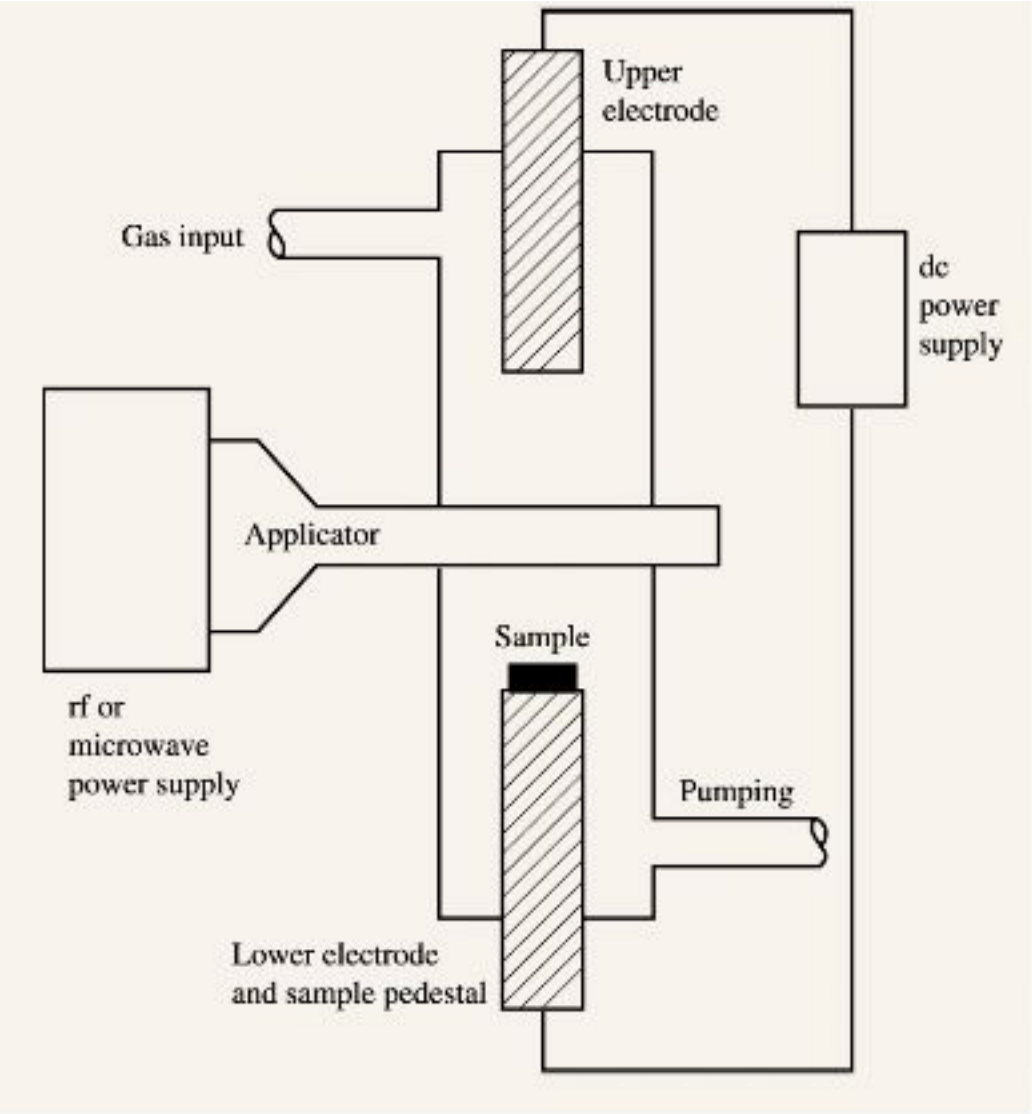

Figure 1

Schematic of an inductively coupled rf or microwave plasma oxidation system. From [10], adapted/reproduced with permission.

IBM Journal of Research and Development
Volume 43, Numbers 1/2, 1999
Plasma processing

Table of contents: HTML ASCII
This article: HTML ASCII
Copyright info

Plasma-assisted oxidation, anodization, and nitridation of silicon - References

by D. W. Hess

References

1. 1. C. J. Dell'Oca, D. L. Pulfrey, and L. Young, "Anodic Oxide Films," *Physics of Thin Films,* Vol. 6, H. Francombe and R. W. Hoffmann, Eds., Academic Press, Inc., New York, 1971, pp. 1-79.
2. J. F. O'Hanlon, "Gas Discharge Anodization," *Oxides and Oxide Films,* Vol. 5, A. K. Vijh, Ed., Marcel Dekker, New York, 1977, pp. 105-166.
3. A. T. Fromhold, Jr., and J. M. Baker, "Oxide Growth in an rf Plasma," *J. Appl. Phys.* **51,** 6377-6392 (1980).
4. S. Gourrier and M. Bacal, "Review of Oxide Formation in a Plasma," *Plasma Chem. Plasma Proc.* **1,** 217-232 (1981).
5. P. Friedel and S. Gourrier, "Review of Oxidation Processes in Plasmas," *J. Phys. Chem. Solids* **44,** 353-364 (1983).
6. A. Reisman, "Assisted Oxidation and Annealing in VLSI and ULSI," *Semiconductor Silicon,* H. Huff, T. Abe, and B. Kolbesen, Eds., The Electrochemical Society, Inc., Pennington, NJ, 1986, pp. 364-378.
7. S. Taylor, J. F. Zhang, and W. Eccleston, "A Review of the Plasma Oxidation of Silicon and Its Applications," *Semicond. Sci. Technol.* **8,** 1426-1433 (1993).
8. D. W. Hess, "Plasma-Assisted Oxidation and Nitridation of Silicon," *Proceedings of the Symposium on Silicon Nitride and Silicon Dioxide Thin Insulating Films,* V. J. Kapoor and W. D. Brown, Eds., The Electrochemical Society, Inc., Pennington, NJ, 1994, pp. 229-243.
9. J. R. Ligenza, "Silicon Oxidation in an Oxygen Plasma Excited by Microwaves," *J. Appl. Phys.* **36,** 2703-2707 (1965).
10. J. Kraitchman, "Silicon Oxide Films Grown in a Microwave Discharge," *J. Appl. Phys.* **38,** 4323-4330 (1967).
11. A. Kiermasz, W. Eccleston, and J. L. Moruzzi, "Theory of the Growth of SiO_2 in an Oxygen Plasma," *Solid State Electron.* **26,** 1167-1172 (1983).
12. S. Taylor, K. J. Barlow, W. Eccleston, and A. Kiermasz, "Comparison of rf and Microwave Oxidation Systems for the Growth of Thin Oxides at Low Temperatures," *Electron. Lett.* **23,** 309-310 (1987).
13. S. Taylor, W. Eccleston, and K. J. Barlow, "Theory for the Plasma Anodization of Silicon under Constant Voltage and Constant Current Conditions," *J. Appl. Phys.* **64,** 6515-6522 (1988).
14. K. J. Barlow, S. Taylor, W. Eccleston, and A. Kiermasz, "The Low-Temperature Anodization of Silicon in a Gaseous Plasma," *IEEE Trans.*

Electron Devices **ED-36,** 1279-1285 (1989).
15. C. Y. Fu, J. C. Mikkelsen, Jr., J. Schmitt, J. Abelson, J. C. Knights, N. Johnson, A. Barker, and M. J. Thompson, "Microwave Plasma Oxidation of Silicon," *J. Electron. Mater.* **14,** 685-706 (1985).
16. D. W. Hess, "Oxidation of Silicon in Halogenated Atmospheres and Oxidation of Heavily Doped Silicon: Analysis by the Deal-Grove Model," *The Physics and Chemistry of SiO_2 and the Si-SiO_2 Interface,* Vol. 3, J. Z. Massoud, E. H. Poindexter, and C. R. Helms, Eds., The Electrochemical Society, Inc., Pennington, NJ, 1996, pp. 143-159.
17. J. Ruzyllo, A. Hoff, and G. Ruggles, "Evaluation of Thin Oxides Grown by the Atomic Oxygen Afterglow Method," *J. Electron. Mater.* **16,** 373-378 (1987).
18. C. Vinckier, P. Coeckelberghs, G. Stevens, M. Heyns, and S. DeJaegere, "Kinetics of the Silicon Dioxide Growth Process in Afterglows of Microwave-Induced Plasmas," *J. Appl. Phys.* **62,** 1450-1458 (1987).
19. C. Vinckier, P. Coeckelberghs, G. Stevens, and S. DeJaegere, "Oxidation of Silicon in the Afterglow of Microwave Induced Plasmas," *Appl. Surf. Sci.* **30,** 40-46 (1987).
20. Y. Yasuda, S. Zaima, T. Kaida, and Y. Koide, "Formation of Si-SiO_2 Interfaces at Low Temperatures Using Microwave-Excited Plasma," *Appl. Surf. Sci.* **41/42,** 429-432 (1989).
21. Y. Yasuda, S. Zaima, T. Kaida, and Y. Koide, "Mechanisms of Silicon Oxidation at Low Temperatures by Microwave-Excited O_2 Gas and O_2-N_2 Mixed Gas," *J. Appl. Phys.* **67,** 2603-2607 (1990).
22. C. Vinckier and S. DeJaegere, "Yields of the Plasma Oxidation of Silicon by Neutral Oxygen Atoms and Negative Oxygen Atom Ions," *J. Electrochem. Soc.* **137,** 628-631 (1990).
23. D. L. Pulfrey, F. G. M. Hathorn, and L. Young, "The Anodization of Si in an RF Plasma," *J. Electrochem. Soc.* **120,** 1529-1535 (1973).
24. D. L. Pulfrey and J. J. H. Reche, "Preparation and Properties of Plasma-Anodized Silicon Dioxide Films," *Solid State Electron.* **17,** 627-632 (1974).
25. V. Q. Ho and T. Sugano, "Selective Anodic Oxidation of Silicon in Oxygen Plasma," *IEEE Trans. Electron Devices* **ED-27,** 1436-1443 (1980).
26. A. J. Choksi, R. Lal, and A. N. Chandorkar, "Electrical Properties of Silicon Dioxide Grown by Inductively Coupled R. F. Plasma Anodization," *Solid State Electron.* **34,** 765-770 (1991).
27. H. Kuroki, H. Shinno, K. G. Nakamura, M. Kitajima, and T. Kawabe, "Plasma Density Dependence of the Oxidation Rate of Si by In-Situ During Process Rapid Ellipsometry," *J. Appl. Phys.* **71,** 5278-5280 (1992).
28. T. Ueno, T. Akiyama, K. Kuroiwa, and Y. Tarui, "Highly Efficient Generation of High-Energy Photons and Low-Temperature Oxidation of a Crystal Silicon Surface with O^1D Radicals," *Appl. Surf. Sci.* **79/80,** 502-506 (1994).
29. N. Haneji, F. Arai, K. Asada, and T. Sugano, "Anodic Oxidation of Si in Oxygen/Chlorine Plasma," *IEEE J. Solid State Circuits* **SC-20,** 20-25 (1985).
30. A. K. Ray and A. Reisman, "Plasma Oxide FET Devices," *J. Electrochem. Soc.* **128,** 2424-2428 (1981); "The Formation of SiO_2 in an RF Generated Oxygen Plasma. I. The Pressure Range Below 10 mtorr," *J. Electrochem. Soc.* **128,** 2460-2465 (1981); "The Formation of SiO_2 in an RF Generated Oxygen Plasma. II. The Pressure Range Above 10 mtorr," *J. Electrochem. Soc.* **128,** 2466-2472 (1981).
31. K. Eljabaly and A. Reisman, "Growth Kinetics and Annealing Studies of the

`Cathodic' Plasma Oxidation of Silicon," *J. Electrochem. Soc.* **138,** 1064-1070 (1991); "Species Charge and Oxidation Mechanism in the `Cathodic' Plasma Oxidation of Silicon," *J. Electrochem. Soc.* **138,** 1071-1076 (1991).

32. S. A. Nelson and R. A. Buhrman, "Thin Silicon Oxides Grown by Low-Temperature rf Plasma Anodization and Deposition," *Appl. Phys. Lett.* **50,** 1095-1097 (1987).
33. S. A. Nelson, H. D. Hallen, and R. A. Buhrman, "A Structural and Electrical Comparison of Thin SiO_2 Films Grown on Silicon by Plasma Anodization and Rapid Thermal Processing to Furnace Oxidation," *J. Appl. Phys.* **63,** 5027-5035 (1988).
34. Y. Kawai, N. Konishi, J. Watanabe, and T. Ohmi, "Ultra-Low Temperature Growth of High-Integrity Gate Oxide Films by Low-Energy Ion-Assisted Oxidation," *Appl. Phys. Lett.* **64,** 2223-2225 (1994).
35. D. N. Modlin and W. A. Tiller, "Effects of Corona-Discharge-Induced Oxygen Ion Beams and Electric Fields on Silicon Oxidation Kinetics. I. Ion Beam Effects," *J. Electrochem. Soc.* **138,** 1163-1168 (1985); "Effects of Corona-Discharge-Induced Oxygen Ion Beams and Electric Fields on Silicon Oxidation Kinetics. II. Electric Field Effects," *J. Electrochem. Soc.* **132,** 1659-1663 (1985).
36. L. M. Landesberger, D. B. Kao, and W. A. Tiller, "Conformal Two-Dimensional SiO_2 Layers on Silicon Grown by Low Temperature Corona Discharge," *J. Electrochem. Soc.* **132,** 1766-1771 (1988).
37. M. R. Madani and P. K. Ajmera, "Characterization of Silicon Oxide Films Grown at Room Temperature by Point-To-Plane Corona Discharge," *J. Electron. Mater.* **22,** 1147-1152 (1993).
38. J. A. Dagate, J. Schnier, H. H. Harary, C. J. Evans, M. T. Postek, and J. Bennett, "Modification of Hydrogen-Passivated Silicon by a Scanning Tunneling Microscope Operating in Air," *Appl. Phys. Lett.* **56,** 2001-2003 (1990).
39. H. Sugimura and N. Nakagiri, "Fabrication of Silicon Nanostructures Through Scanning Probe Anodization Followed by Chemical Etching," *Nanotechnol.* **6,** 29-33 (1995).
40. A. E. Gordon, R. T. Fayfield, D. D. Litfin, and T. K. Higman, "Mechanisms of Surface Anodization Produced by Scanning Probe Microscopes," *J. Vac. Sci. Technol. B* **13,** 2805-2808 (1995).
41. E. S. Snow, P. M. Campbell, and P. J. McMarr, "AFM-Based Fabrication of Free-Standing Si Nanostructures," *Nanotechnol.* **7,** 434-437 (1996).
42. D. Stievenard, P. A. Fontaine, and E. Dubois, "Nanooxidation Using a Scanning Probe Microscope: An Analytical Model Based on Field Induced Oxidation," *Appl. Phys. Lett.* **70,** 3272-3274 (1997).
43. P. Avouris, T. Hertel, and R. Martel, "Atomic Force Microscope Tip-Induced Local Oxidation of Silicon: Kinetics, Mechanism, and Nanofabrication," *Appl. Phys. Lett.* **71,** 285-287 (1997).
44. D. A. Carl, D. W. Hess, and M. A. Lieberman, "Oxidation of Silicon in an Electron Cyclotron Resonance Oxygen Plasma: Kinetics, Physicochemical, and Electrical Properties," *J. Vac. Sci. Technol. A* **8,** 2924-2930 (1990).
45. S. Kimura, E. Murakami, K. Miyake, T. Warabisako, H. Sunami, and T. Tokuyama, "Low Temperature Oxidation of Silicon in a Microwave-Discharged Oxygen Plasma," *J. Electrochem. Soc.* **132,** 1460-1466 (1985).
46. S. Kimura, E. Murakami, T. Warabisako, and H. Sunami, "Microwave-Discharge Plasma Oxidation of Silicon in a Cusp Magnetic Field," *J.*

Electrochem. Soc. **135,** 2009-2012 (1988).
47. S. Kimura, E. Murakami, K. Miayake, T. Warabisako, E. Mitani, and H. Sunami, "An ^{18}O Study of Oxygen Exchange Phenomena During Microwave-Discharge Plasma Oxidation of Silicon," *J. Appl. Phys.* **63,** 4655-4660(1988).
48. B. E. Deal and A. S. Grove, "General Relationship for the Thermal Oxidation of Silicon," *J. Appl. Phys.* **36,** 3770-3778 (1965).
49. N. Cabrera and N. Mott, "Theory of the Oxidation of Metals," *Rept. Prog. Phys.* **12,** 163-184 (1948).
50. G. T. Salbert, D. K. Reinhard, and J. Asmussen, "Oxide Growth on Silicon Using a Microwave Electron Cyclotron Resonance Oxygen Plasma," *J. Vac. Sci. Technol. A* **8,** 2919-2923 (1990).
51. D. A. Carl, D. W. Hess, M. A. Lieberman, T. D. Nguyen, and R. Gronsky, "Effects of dc Bias on the Kinetics and Electrical Properties of Silicon Dioxide Grown in an Electron Cyclotron Resonance Plasma," *J. Appl. Phys.* **70,** 3301-3313 (1991).
52. D. R. Wolters and A. T. A. Zegers-van Duynhoven, "Kinetics of Dry Oxidation of Silicon. I. Space-Charge-Limited Growth," *J. Appl. Phys.* **65,** 5126-5133 (1989); "Kinetics of Dry Oxidation of Silicon. II. Conditions Affecting the Growth," *J. Appl. Phys.* **65,** 5134-5141 (1989).
53. J. Joseph, Y. Z. Hu, and E. A. Irene, "A Kinetics Study of the Electron Cyclotron Resonance Plasma Oxidation of Silicon," *J. Vac. Sci. Technol. B* **10,** 611-617 (1992).
54. T. G. Mills and F. A. Kroger, "Electrical Conduction at Elevated Temperatures in Thermally Grown Silicon Dioxide Films," *J. Electrochem. Soc.* **120,** 1582-1586 (1973).
55. Y. Z. Hu, Y. Q. Wang, M. Li, J. Joseph, and E. A. Irene, "In Situ Investigation of Temperature and Bias Dependent Effects on the Oxide Growth of Si and Ge in an Electron Cyclotron Resonance," *J. Vac. Sci. Technol. A* **11,** 900-904 (1993).
56. P. R. Lefebvre and E. A. Irene, "Comparison of Si and GaAs/Interfaces Resulting from Thermal and Plasma Oxidation," *J. Vac. Sci. Technol. B* **15,** 1173-1181 (1997).
57. Y. Z. Hu, J. Joseph, and E. A. Irene, "In Situ Spectroscopic Ellipsometry Study of the Electron Cyclotron Resonance Plasma Oxidation of Silicon and Interfacial Damage," *Appl. Phys. Lett.* **59,** 1353-1355 (1991).
58. S. R. Kaluri and D. W. Hess, "Constant Current N_2O Plasma Anodization of Silicon," *J. Electrochem. Soc.* **144,** 2200-2205 (1997).
59. A. Kazor and I. W. Boyd, "Ozone-Induced Rapid Low Temperature Oxidation of Silicon," *Appl. Phys. Lett.* **63,** 2517-2519 (1993).
60. I. S. Goh, S. Hall, W. Eccleston, J. F. Zhang, and K. Werner, "Interface Quality of SiGe Oxide Prepared by RF Plasma Anodisation," *Electron. Lett.* **30,** 1988-1989 (1994).
61. I. S. Goh, J. F. Zhang, S. Hall, W. Eccleston, and K. Werner, "Plasma Oxidation of Si and SiGe," *Microelectron. Eng.* **28,** 221-224 (1995).
62. P. W. Li, H. K. Liou, E. S. Yang, S. S. Iyer, T. P. Smith III, and Z. Lu, "Formation of Stoichiometric SiGe Oxide by Electron Cyclotron Resonance Plasma," *Appl. Phys. Lett.* **60,** 3265-3267 (1992).
63. P. W. Li and E. S. Yang, "SiGe Gate Oxide Prepared at Low Temperature in an Electron Cyclotron Resonance Plasma," *Appl. Phys. Lett.* **63,** 2938-2940 (1993).
64. R. C. Frye, J. J. Kumler, and C. C. Wong, "Investigation of Surface

Passivation of Amorphous Silicon Using Photothermal Deflection Spectroscopy," *Appl. Phys. Lett.* **50,** 101-103 (1987).
65. P. Danesh, "Post-Deposition Oxygen Plasma Treatment of a-Si:H," *Thin Solid Films* **202,** L5-L7 (1991).
66. S. R. Kaluri, R. S. Howell, D. W. Hess, and M. K. Hatalis, "Helical Resonator Plasma Oxidation of Amorphous and Polycrystalline Silicon for Flat Panel Displays," *Flat Panel Display Materials II,* M. K. Hatalis, J. Kanicki, C. J. Summers, and F. Funada, Eds., Mater. Res. Soc. Symp. Proc. 424, 165-170 (1997).
67. T.-H. Ihn, S.-W. Lee, B.-I. Lee, Y.-C. Jeon, and S.-K. Joo, "ECR Plasma Oxidation of Amorphous Silicon for Improvement of the Interface State in a Poly Silicon Thin Film Transistor," *Flat Panel Display Materials II,* M. K. Hatalis, J. Kanicki, C. J. Summers, and F. Funada, Eds., Mater. Res. Soc. Symp. Proc. 424, 189-195 (1997).
68. J.-Y. Lee, C.-H. Han, and C.-K. Kim, "High Performance Low Temperature Polysilicon Thin Film Transistor Using ECR Plasma Thermal Oxide as Gate Insulator," *IEEE Electron Device Lett.* **15,** 301-303 (1994).
69. J.-Y. Lee, C.-H. Han, C.-K. Kim, and B.-K. Kim, "Effects of Electron Cyclotron Resonance Plasma Thermal Oxidation on the Properties of Polycrystalline Silicon Films," *Appl. Phys. Lett.* **67,** 1880-1882 (1995).
70. B.-H. Min, C.-M. Park, J.-H. Jun, B.-S. Bae, and M.-K. Han, "Performance of Poly-Si TFTs with Double Gate Oxide Layers," *Flat Panel Display Materials II,* M. K. Hatalis, J. Kanicki, C. J. Summers, and F. Funada, Eds., Mater. Res. Soc. Symp. Proc. 424, 171-176 (1997).
71. A. A. Bright, J. Batey, and E. Tierney, "Low-Rate Plasma Oxidation of Si in a Dilute Oxygen/Helium Plasma for Low-Temperature Gate Quality Si/SiO_2 Interfaces," *Appl. Phys. Lett.* **58,** 619-621 (1991).
72. G. Lucovsky, T. Yasuda, Y. Ma, S. Habermehl, S. S. He, and D. J. Stephens, "Low Temperature Plasma-Assisted Oxidation and Thin-Film Deposition Processes for Forming Device-Quality SiO_2/Si and Composite Dielectric-SiO_2/Si Heterostructures," *Thin Solid Films* **220,** 38-44 (1992).
73. A. Reisman, M. Berkenblit, A. K. Ray, and C. J. Merz, "Nitridation of Silicon in a Multiwafer Plasma System," *J. Electron. Mater.* **13,** 505-521 (1984).
74. S. S. Wong and W. G. Oldham, "A Multiwafer Plasma System for Anodic Nitridation and Oxidation," *IEEE Electron Device Lett.* **EDL-5,** 175-177 (1984).
75. M. Hirayama, T. Matsukawa, H. Arima, Y. Ohno, N. Tsubouchi, and H. Nakata, "Plasma Anodic Nitridation of Silicon in N_2-H_2 System," *J. Electrochem. Soc.* **131,** 663-666 (1984).
76. M. Hirayama, T. Matsukawa, H. Arima, Y. Ohno, and H. Nakata, "Growth Mechanism of Silicon Plasma Anodic Nitridation," *J. Electrochem. Soc.* **132,** 2494-2497 (1985).
77. A. Ermolieff, P. Bernard, S. Marthon, and J. Camargo DaCosta, "Nitridation of Si(100) Made by Radio Frequency Plasma as Studied by In-Situ Angular Resolved X-Ray Photoelectron Spectroscopy," *Dielectric Layers in Semiconductors: Novel Technologies and Devices,* G. G. Bentini, Ed., Cedex, France, 1986, pp. 83-94.
78. J. L. Pyle, T. G. Ruskell, R. K. Workman, X. Yao, and D. Sarid, "Growth of Silicon Nitride by Scanned Probe Lithography," *J. Vac. Sci. Technol. B* **15,** 38-39 (1997).
79. P. Chen, K. Y. Hsu, J. Lin, and H. Hwang, "Characterization of Ultrathin Dielectrics Grown by Microwave Afterglow Oxygen and N_2O Plasma," *Jpn. J.*

Appl. Phys. **34,** 973-977 (1995).
80. Y. Saito, "Oxynitridation of Silicon by Remote-Plasma Excited Nitrogen and Oxygen," *Appl. Phys. Lett.* **68,** 800-802 (1996).
81. P. J. Tobin, Y. Okada, S. A. Ajuria, V. Lakhotia, W. A. Feil, and R. I. Hegde, "Furnace Formation of Silicon Oxynitride Thin Dielectrics in Nitrous Oxide (N_2O): The Role of Nitric Oxide (NO)," *J. Appl. Phys.* **75,** 1811-1817 (1994).
82. K. A. Ellis and R. A. Buhrman, "Furnace Gas-Phase Chemistry of Silicon Oxynitridation in N_2O," *Appl. Phys. Lett.* **68,** 1696-1698 (1996).
83. K. Koh, H. Nimi, and G. Lucovsky, "Reaction Pathways for Nitrogen Incorporation at Si-SiO_2 Interfaces," *Amorphous and Crystalline Insulating Thin Films--1996,* W. L. Warren, R. A. B. Devine, M. Matsumura, S. Cristoloveanu, Y. Homma, and J. Kanicki, Eds., *Mater. Res. Soc. Symp. Proc.* **446,** 267-272 (1997).
84. S. R. Kaluri and D. W. Hess, "Constant Current N_2O Plasma Anodization of Silicon," *J. Electrochem. Soc.* **144,** 2200-2205 (1997).
85. Z. H. Lu, S. P. Tay, R. Cao, and P. Pianetta, "The Effect of Rapid Thermal N_2O Nitridation on the Oxide/Si (100) Interface Structure," *Appl. Phys. Lett.* **67,** 2836-2838 (1995).
86. S. R. Kaluri and D. W. Hess, "Nitrogen Incorporation in Thin Silicon Oxides in a N_2O Plasma--Effects of Processing Conditions," *J. Electrochem. Soc.* **145,** 662-668 (1998).
87. S. R. Kaluri, "Plasma-Assisted Nitrogen Incorporation in Thin Gate Dielectrics," Ph.D. Thesis, Lehigh University, Bethlehem, PA, 1997.
88. M. Bhat, L. K. Han, D. Wristers, J. Yan, D. L. Kwong, and J. Fulford, "Effect of Chemical Composition on the Electrical Properties of NO^- Nitrided SiO_2," *Appl. Phys. Lett.* **66,** 1225-1227 (1995).
89. T. Arakawa, R. Matsumoto, and A. Kita, "Effect of Nitrogen Profile on Tunnel Oxynitride Degradation with Charge Injection Polarity," *Jpn. J. Appl. Phys.* **35,** 1491-1495 (1996).
90. R. Kraft, T. P. Schneider, W. W. Dostalik, and S. Hattangady, "Surface Nitridation of Silicon Dioxide with a High Density Nitrogen Plasma," *J. Vac. Sci. Technol. B* **15,** 967-970 (1997).
91. D. T. Grider, S. V. Hattangady, R. Kraft, P. E. Nicollian, J. Kuehne, G. Brown, S. Aur, R. H. Eklund, and M. F. Pas, "A 0.18μm CMOS Process Using Nitrogen Profile-Engineered Gate Dielectrics," *VLSI Tech. Digest,* pp. 47-48 (1997).
92. J.-W. Lee, N.-I. Lee, and C.-H. Han, "Characteristics of Polysilicon Thin-Film Transistor with Thin-Gate Dielectric Grown by Electron Cyclotron Resonance Nitrous Oxide Plasma," *IEEE Electron Device Lett.* **18,** 172-174 (1997).
93. N.-I. Lee, J.-W. Lee, S.-H. Hur, H.-S. Kim, and C.-H. Han, "Highly Reliable Polysilicon Oxide Grown by Electron Cyclotron Resonance Nitrous Oxide Plasma," *IEEE Electron Device Lett.* **18,** 486-488 (1997).
94. J.-W. Lee, N.-I. Lee, S.-H. Hur, and C.-H. Han, "Oxidation of Silicon Using Electron Cyclotron Resonance Nitrous Oxide Plasma and Its Application to Polycrystalline Silicon Thin Film Transistors," *J. Electrochem. Soc.* **144,** 3283-3287 (1997).
95. C. S. Lai, T. F. Lei, and C. L. Lee, "The Characteristics of Polysilicon Oxide Grown in Pure N_2O," *IEEE Trans. Electron Devices* **43,** 326-331 (1996).
96. A. Masuda, A. Morimoto, M. Kumeda, and T. Shimizu, "Novel Oxidation Process of Hydrogenated Amorphous Silicon Utilizing Nitrous Oxide Plasma,"

Appl. Phys. Lett. **61,** 816-818 (1992).

97. A. Masuda, I. Fukushi, Y. Yonezawa, T. Minamikawa, A. Morimoto, M. Kumeda, and T. Shimizu, "Spectroscopic Study on N_2O-Plasma Oxidation of Hydrogenated Amorphous Silicon and Behavior of Nitrogen," *Jpn. J. Appl. Phys.* **32,** 2794-2802 (1993).
98. H. Yokomichi, A. Masuda, Y. Yonezawa, and T. Shimizu, "N_2-Plasma-Nitridation Effects on Porous Silicon," *Thin Solid Films 281-282,* 568-571 (1996).

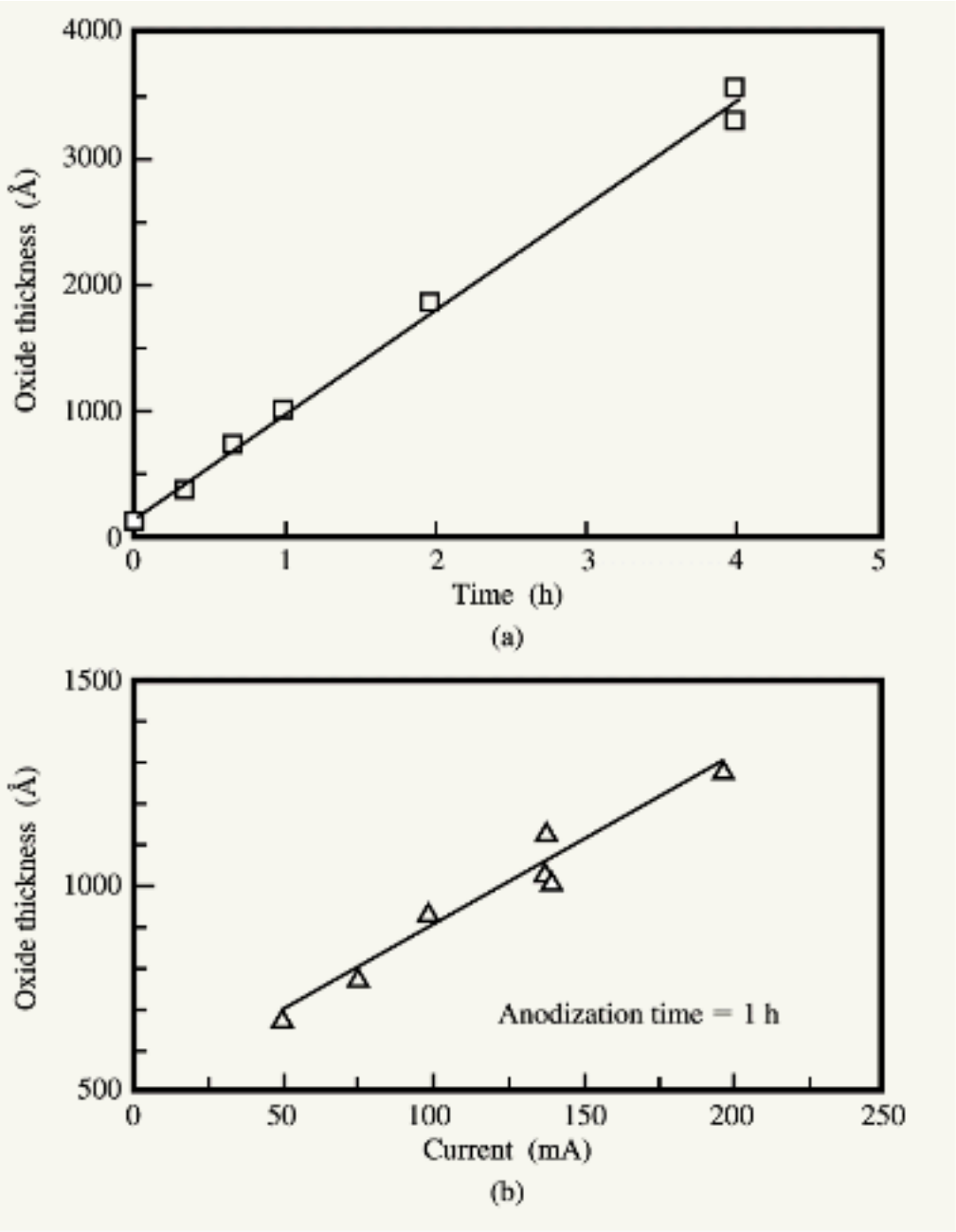

Figure 2

(a) Silicon oxide thickness vs. oxidation time for microwave oxidation at ~10 mA/cm^2; (b) silicon oxide thickness vs. anodization current density. From [15], reproduced with permission; © 1985 IEEE.

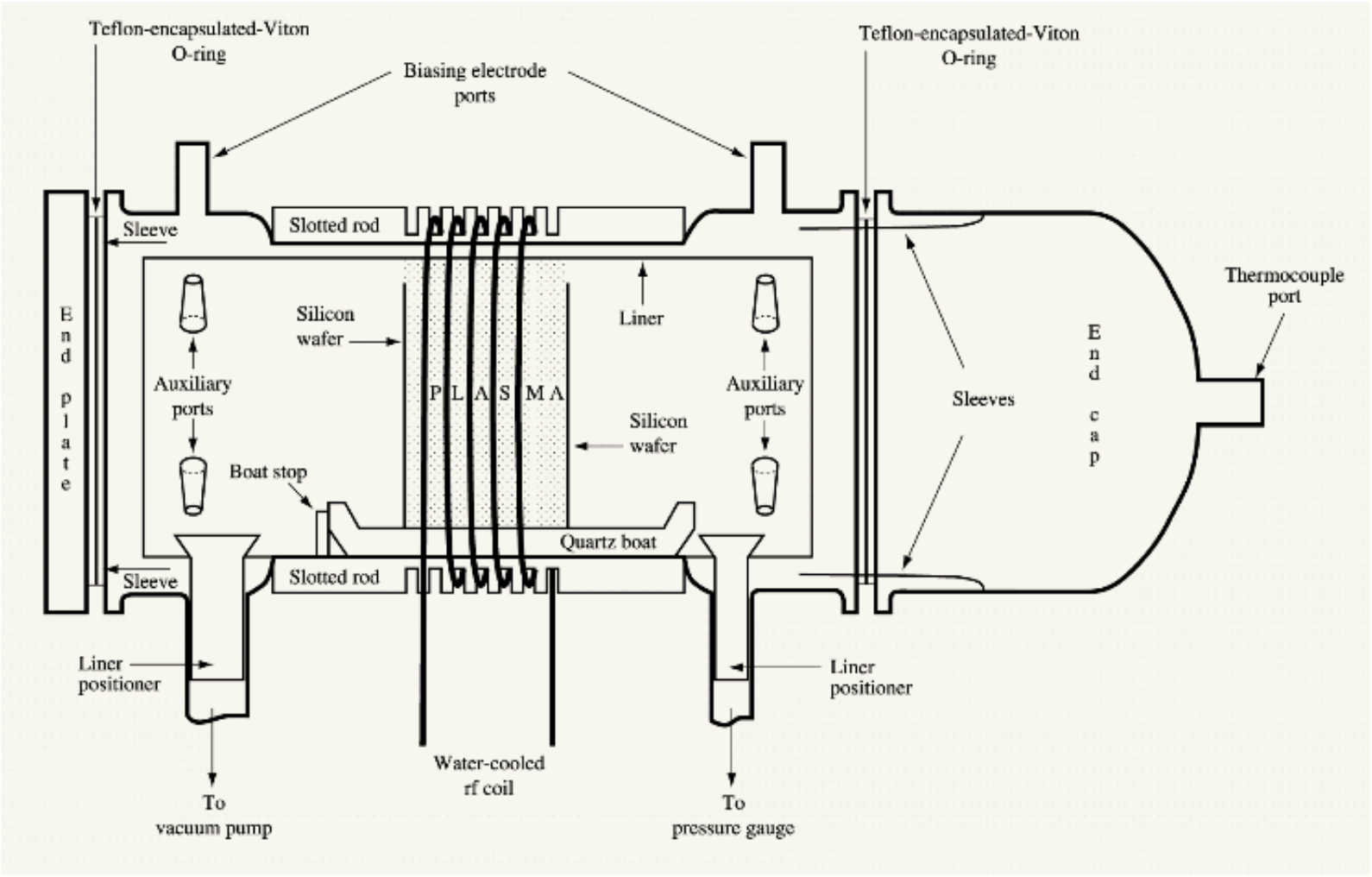

Figure 3

Reactor configuration for cathodic plasma-assisted oxidation. From [31], reproduced with permission of The Electrochemical Society, Inc.

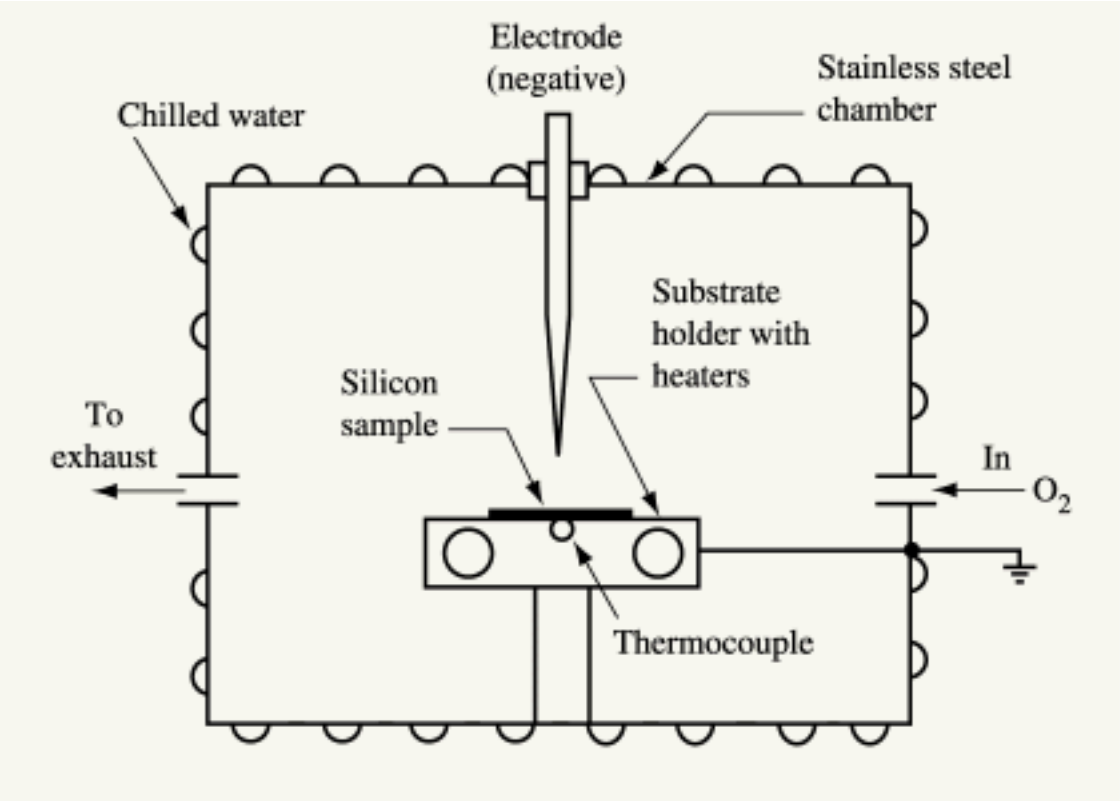

Figure 4

Corona discharge plasma-assisted oxidation system. From [37], reproduced with permission; © 1993 IEEE.

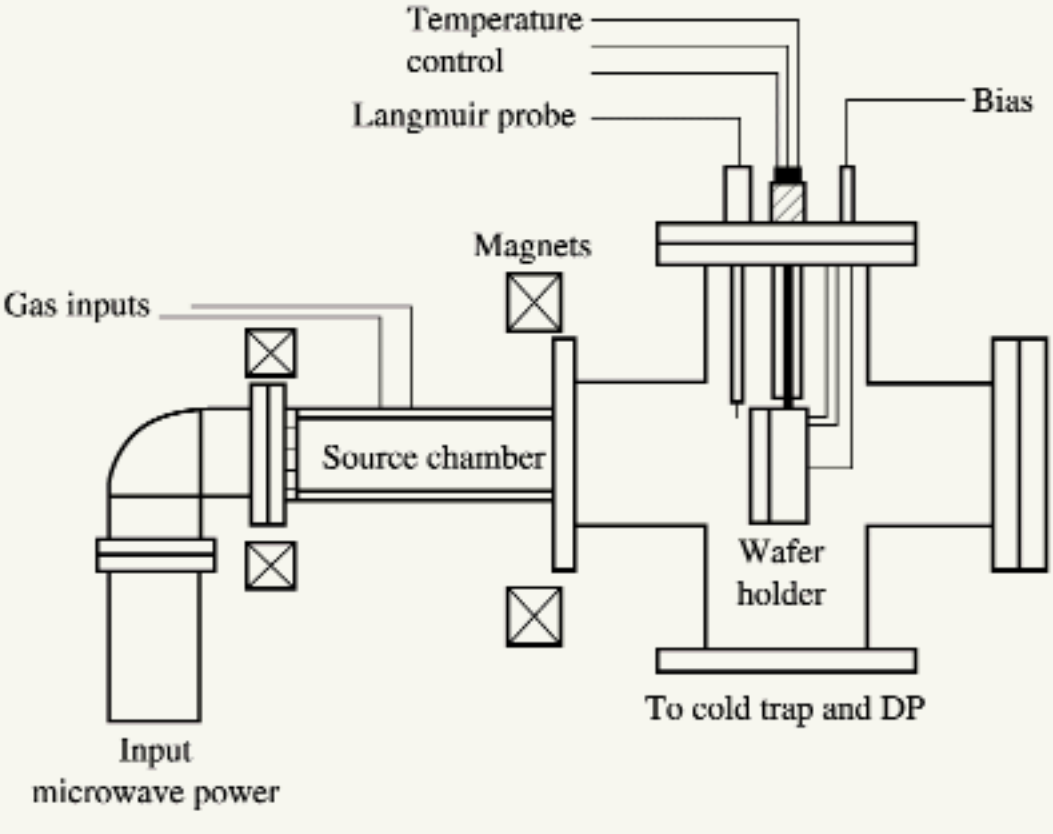

Figure 5

Schematic of electron cyclotron resonance (ECR) plasma-assisted oxidation system. From [44], reproduced with permission.

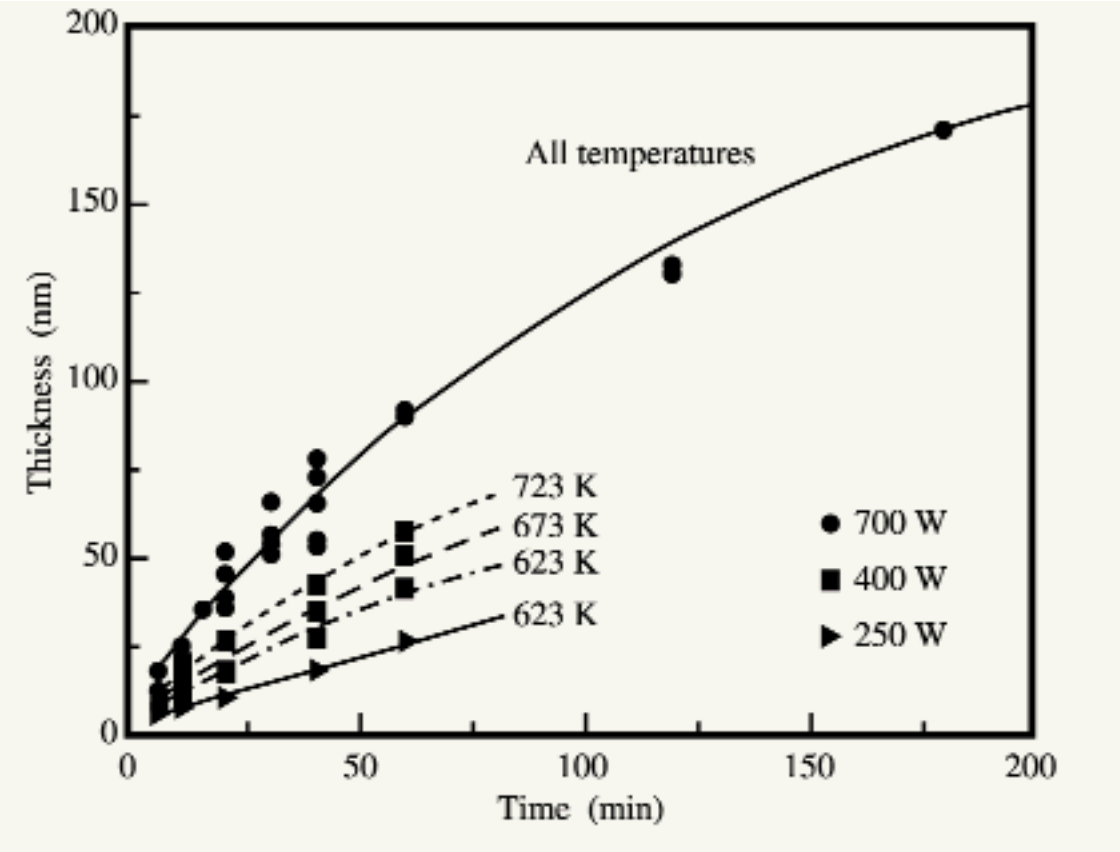

Figure 6

Silicon oxide thickness vs. ECR oxidation time at 1 mTorr O_2; power levels are those applied to the microwave source. From [44], adapted/reproduced with permission.

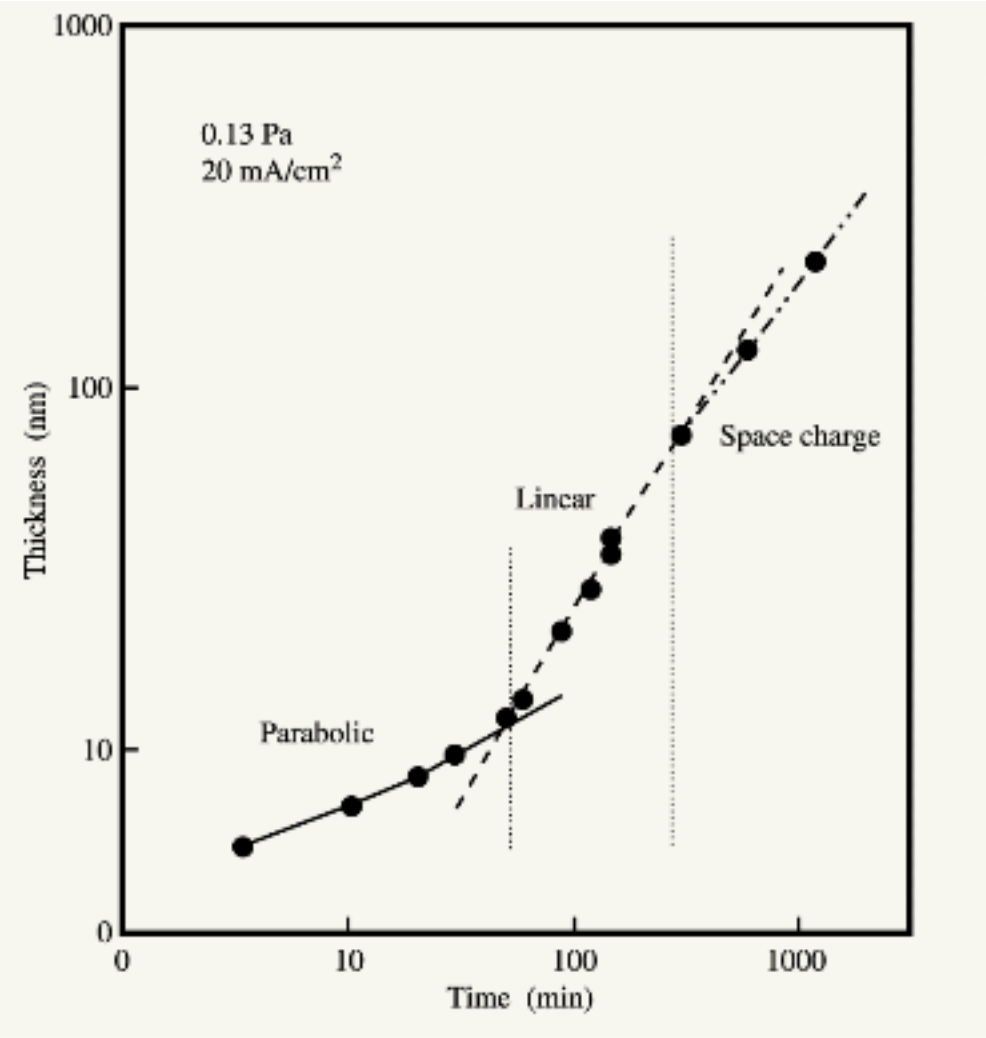

Figure 7

Oxide thickness vs. oxidation time for constant-current plasma-assisted anodization of silicon at 350°C. From [51], adapted/ reproduced with permission.

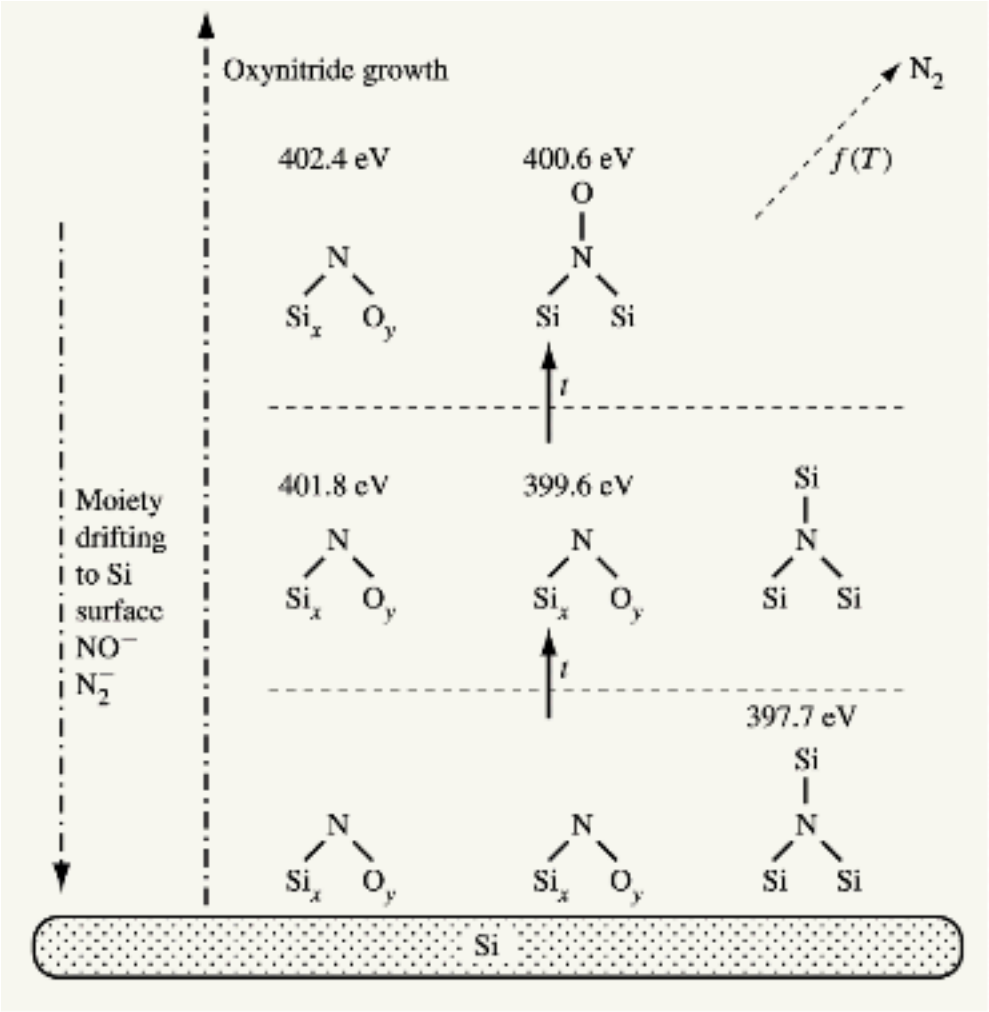

Figure 8

Schematic of the evolution of nitrogen-bonding structures as a function of plasma-assisted oxidation time. The differences in depicted sizes relate to the atomic concentrations of nitrogen. The binding energies shown are for N 1*s* in each bonding structure. From [84], reproduced with permission from The Electrochemical Society, Inc.

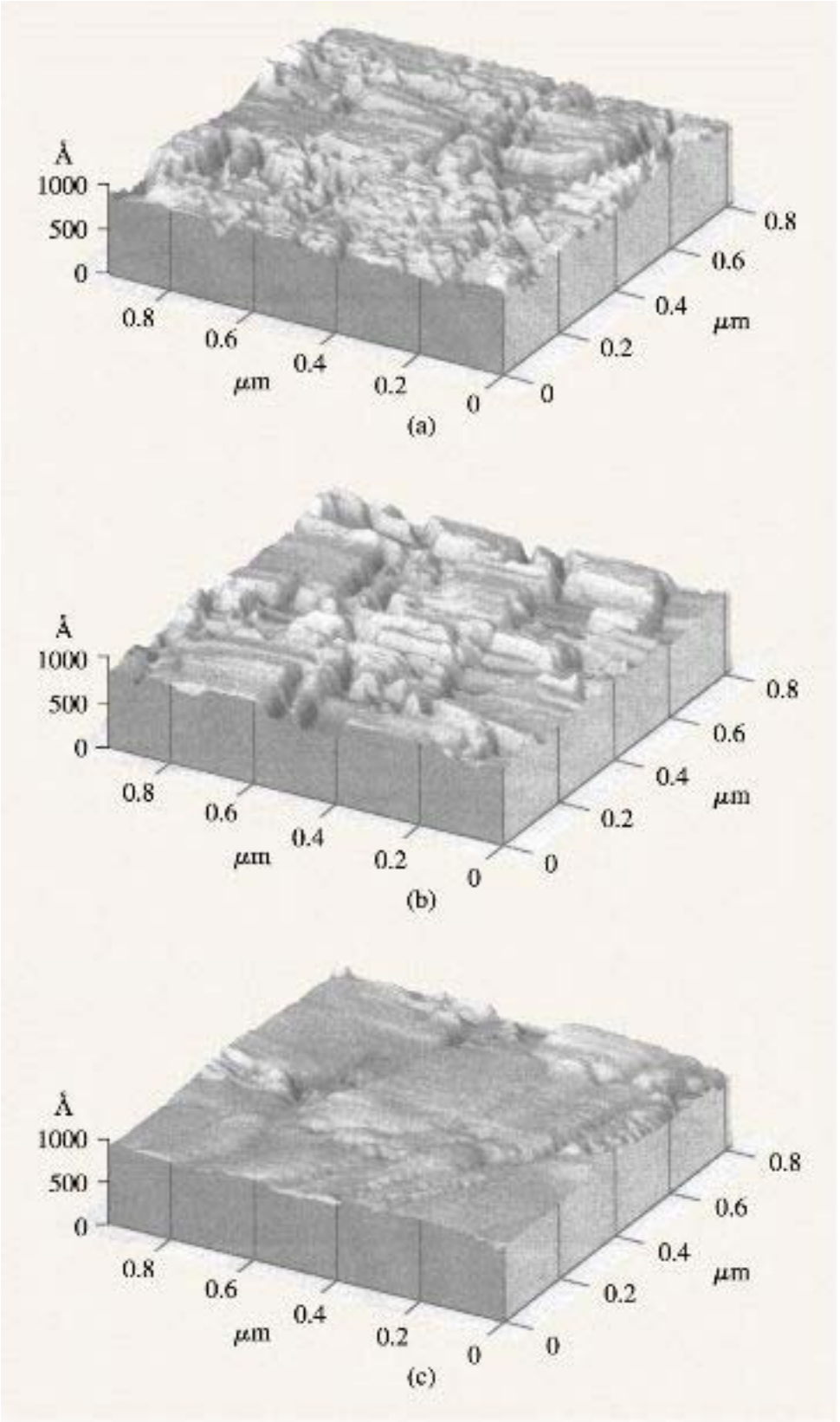

Figure 9

AFM images of polycrystalline silicon films deposited using SiH_4 source gas in the amorphous phase at 550°C, annealed at 600°C for 24 h, n^+-doped using phosphorus solid diffusion at 950°C, and processed (a) without oxidation, (b) with thermal oxidation at 900°C in O_2, and (c) with N_2O ECR plasma-assisted oxidation at 400°C and 2 mTorr. Before measurement, the oxide films were

900°C in O_2, and (c) with N_2O ECR plasma-assisted oxidation at 400°C and 2 mTorr. Before measurement, the oxide films were removed completely in a 50:1 HF solution. The average rms values of surface roughness of (a), (b), and (c) were 6.4, 9.4, and 4.6 nm, respectively. From [94], reproduced with permission from The Electrochemical Society, Inc.